SOLID-STATE DRIVE FOR SOLAR WATER PUMPS

A Thesis Submitted
In Partial Fulfilment of the Requirements
for the Degree of
MASTER OF TECHNOLOGY

By
M. K. BALACHANDER

to the
DEPARTMENT OF ELECTRICAL ENGINEERING
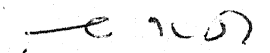## INDIAN INSTITUTE OF TECHNOLOGY, KANPUR
AUGUST, 1980

CERTIFICATE

Certified that this work "Solid-State Drive for Solar
Water Pumps" by M.K. Balachander is carried out under our
supervision and is not submitted elsewhere for a degree.

(Dr. S.R. Doradla)
Assistant Professor

(Dr. G.K. Dubey)
Professor

Department of Electrical Engineering
Indian Institute of Technology
Kanpur,   INDIA.

ACKNOWLEDGEMENT

CONTENTS

LIST OF FIGURES

ABSTRACT

With the rapid depletion of fossil fuels, the need for an alternative source of energy has become a necessity. In recent times, there has been an all round effort to tap the natural, abundant solar energy for several applications including rural water pumping. With the rapid development of semiconductor technology, solar water pump of about 1 kw for rural applications is presently considered for development in India. This thesis is concerned with the study and development of a simple, economical, efficient and reliable solid-state drive for a solar water pump besides reviewing other possible solid-state drives.

Among different solid state drives, the single-phase squirrel cage induction motor-current source inverter is quite competitive and ideally suited for such applications. step-up chopper is proposed to interpose between the solar cell voltage source and the inverter especially in times of low solar radiation levels. The chopper and the inverter were built and tested on a single-phase induction motor in the laboratory. Due to non-availability of solar cell array and pump, actual field test could not be undertaken.

The single-phase induction motor fed by current source inverter is analysed for torque-speed characteristics using equivalent circuit model. The actual torque-speed characteristics, are also obtained from the experimental set-up in the

laboratory. There is a close agreement between the experimental results and analytical results obtained using only the fundamental component of motor current.

CHAPTER 1

INTRODUCTION

Fossil fuels, which have been the main source of energy, are being consumed at an alarmingly increasing rate. This rate of consumption is bound to totally deplete these fuels in not too distant future. Solar energy, which is abundantly available is presently being considered as a potential energy source for several applications such as water and air heating, cold storage, grain drying, water pump etc. In India, where agriculture is the occupation of majority of the people, the solar energy, if utilized for irrigation will boost farm production. Therefore, there is an increasing awareness on the part of planners, to give top priority for developing a water pump. With the rapid development in semiconductor technology, the water pump run by an electric drive may prove to be more economical and efficient over the mechanical type.

The object of the present study is to develop a simple, reliable, economical drive for a solar water pump.

Chapter 2 describes the solar energy conversion and storage. Also it describes four possible motor drives for a solar pump and concludes with the choice of single phase inverter fed induction motor as the most desirable drive .

Chapter 3 describes the various types of 1-ϕ inverters and a modified parallel inverter is chosen for the present drive due to economic considerations. A step-up chopper which is needed

for keeping the input voltage to the inverter, constant, especially under low solar radiation level, is described and its working is explained.

In Chapter 4, the firing circuit required for both chopper and inverter is described. The important considerations for the successful operation of the complete circuit are also incorporated in the control circuit.

In Chapter 5, the current source inverter with the 1- induction motor as load is analysed for the current waveforms during different modes. Furthermore, a method of calculating torque-speed characteristics of the single-phase induction motor taking into account the effect of saturation of the magnetizing inductance has been presented. The predicted results are verified experimentally.

In Chapter 6, conclusions are drawn and suggestions for future investigations are mentioned.

CHAPTER II

DIFFERENT MOTOR DRIVE CONFIGURATIONS FED BY
SOLAR POWER

2.1 INTRODUCTION

Energy, without which both commerce and industry will come to standstill, comes from fossil fuels like coal, oil etc, and Tidal, Geothermal and Nuclear power sources. Fossil fuel resources are now being consumed at an enormous and continuously increasing rate. Once used, these are replinished forever.

Nuclear power source, which can provide power level at the present world consumption for a very long time, has waste products to be disposed which will create health hazards and a lot of precautions have to be taken against it. Thus an alternative power source which is more permanent and safe is found in solar energy. Solar energy is readily available, well distributed, inexhaustible for all practical purposes and has no polluting effects upon the environments when converted and utilized (1) . The solar energy intercepted by the earth and converted at 10% efficiency could provide the same power which is consumed now, perpectually (2).

Solar energy is intermittent, hence the energy has to be used directly. Alternatively, the energy can be stored and used later, when the sun is not shining. The direct conversion of solar energy is achieved by using collectors. The sun's radiation as ordinarily received is not hot enough to be of much technical use. It must be concentrated from a large area onto a small heating surface, or it must be retained in a heat trap so that the heated object does not lose its heat rapidly. This type of collector, called the focussing type, requires direct sunlight and it must be movable, to follow the sun. The second type called the non-focussing collector, cannot give such high temperature as the first. However, they are not restricted to clear sunny days. They can be used in bright cloudy weather too. More-over, they need not be moved (3).

The solar energy can also be stored in the form of (i) Potential energy, (ii) Heat energy, (iii) Electrical energy. It has been claimed that higher efficiency can be achieved if stored in electrical form (3) . Solar cells are used to convert solar power to electrical power. Solar batteries consist of an array of solar cells. A solar cell is made by a single crystal of silicon, sandwiched in between layers with impurities of trivalent boron and pentavalent arsenic to give p-n junction. It can convert 10-15% of the solar energy directly into electricity without the chemical

consumption of any material. There are several factors
which limit the efficiency to the above said value. Some of
the factors are as follows :

a)   Loss of radiation energy through reflection from silicon
     surface

b)   Losses through recombination processes

c)   Dissipation of a part of electrical energy within the cell

d)   Losses arising from the fact that not all the radiation
     from the sun is in a wavelength region that will provide
     photons with an energy, sufficient to be effective in
     the needed process, while some photons have too much
     energy which is lost as heat (3).

In future, solar power stations would be built in the
vicinity of farms, tapping the solar energy through large
number of solar cell arrays. This power will be made available
for agricultural purposes.

With the improvement in semiconductor technology, it is
possible to achieve still higher efficiency with the solar
cells. Furthermore, the large scale production of solar cells
can lower the cost.

The solar energy, at about 10% efficiency can deliver as
much power as is needed now. This power can be used for
various applications such as water heating, house heating,
bakery, distillation, refrigeration and air conditioning,
cooking, furnace, mechanical power, pumps, turbines etc. Among

the possible uses of solar energy, the lifting of water
for drinking or irrigational purposes is of interest in dry
regions and other rural areas. Requirements of small scale
irrigation and domestic use are well within the reach of solar
energy pumps.

India, being essentially an agricultural country with
70% of the population living in rural areas, require very less
energy. According to statistics (4) , the average power
required in villages is 150 kw hr for energizing irrigation
pumps, for lighting, for cooking etc. As the villages are
widely dispersed from the industrial belt, it is most un-
economical to electrify them. Thus solar energy offers a
viable solution. If the solar energy could be converted to
mechanical energy to drive irrigation pumps and/or to light
homes, the rural scene in India would have a new future with
a boost to agricultural production.

It has been calculated (4) that only 25% of the culti-
vation land is irrigated. Of this, 50% is served by tube-
wells, ponds or such minor irrigation schemes. Due to the
present oil crisis, the need for alternative energy has risen
and development and fabrication of solar pumps have received
top priority in India. Thus the main emphasis in the India
Solar Energy programme is on

a)   research and development of 2-5 hp solar pumps, with
       choice of either using it as   water pump and when
       not required, as a generator for lighting, etc.

b) development and installation of 19-100 kw solar power plants.

In this thesis, a small pump drive is proposed for possible application in rural agriculture which is pertaining to the first part mentioned above. The second part being of large scale application is not the subject of the present study.

A solar water pump, in general, requires a motive force to drive it. The motive power consists of three main parts : (i) Collector, (ii) Storage device, (iii) Motor drive. The first two parts are considered in the earlier paragraphs. Before the motor drive is discussed, it would be in order to present some details about various types of pumps.

An important factor which is to be considered before using the solar energy, is the economic factor. The system must be competitive with the prevailing costs of power stations. The first economic characteristic of most existing solar equipment is the combination of high initial investing costs and low operating costs. Since little or no purchased energy is consumed, the operating cost for solar equipment can be negligible, or atleast considerably lower than that of fuel burning or power using device. And as the less expensive fuels are depleted, and cost of pollution free power station go up, the economic justification of alternate power sources increases.

2.2 CENTRIFUGAL PUMPS

Solar pumps now-a-days are finding widespread use in irrigation. The irrigation pumps, which play an important part in making vast areas of land agriculturally productive, take water from surface sources or sub-surface sources and pump it to the point of application. Centrifugal pumps are commonly used for irrigation. Table I shows different pumps and their important features and pump curves are shown in Fig.2.1.

The prime movers used in irrigation installations are (i) Diesel engines, (ii) Gas engines, and (iii) Electric motors. The use of electric motors is limited only to places where power supply is available. In India, the power supply distribution to all the cultivation land is a formidable task on the part of the planners. Therefore, diesel and gas engines are extensively used for pumping water either from surface or from subsurface to farms. Because of the recent oil crisis, the price of gas and diesel is increasing year by year. The supply of fuel to the farmers is not guaranteed, which will affect the farm production. Thus, in India, solar energy has indeed much relevance.

2.3 SOLAR POWERED DRIVES

Electric motors are the most economical primemovers if reliable source of electric power is available and when the cost of bringing it to the pumping station is not prohibitive. Four schemes, using solar power to run a centrifugal pump,

Table I : Different centrifugal pumps and their features

CLASS	TYPE	HEAD ft	REMARKS
Propellar pumps	a) Vertical single stage	Low heads upto 30 ft	Used mainly for irrigation and drainage
	b) Horizontal axial flow	Very low heads upto 15 ft	Used mainly for pumping large volumes against low heads
Volute pumps	Vertical, Horizontal, End Suction, Bottom Suction	Total head exceeds 45 ft	Used to pump from surface sources and are mounted either in pits or on slabs or floors depending on the application
Deep well Turbine pump	Vertical shaft single suction	High heads (around 100 ft)	Used primarily for irrigation to pump water from subsurface source into distribution system
Submersible turbine pump	Vertical or horizontal	High heads (around 100 ft)	Used for high head applications where long intermediate shafts are undesirable
Portable pumps	"	Low heads (around 30 ft)	Used both in drainage and irrigation work. Such pumps are of small capacity and economical. Can be used as submersible type also.
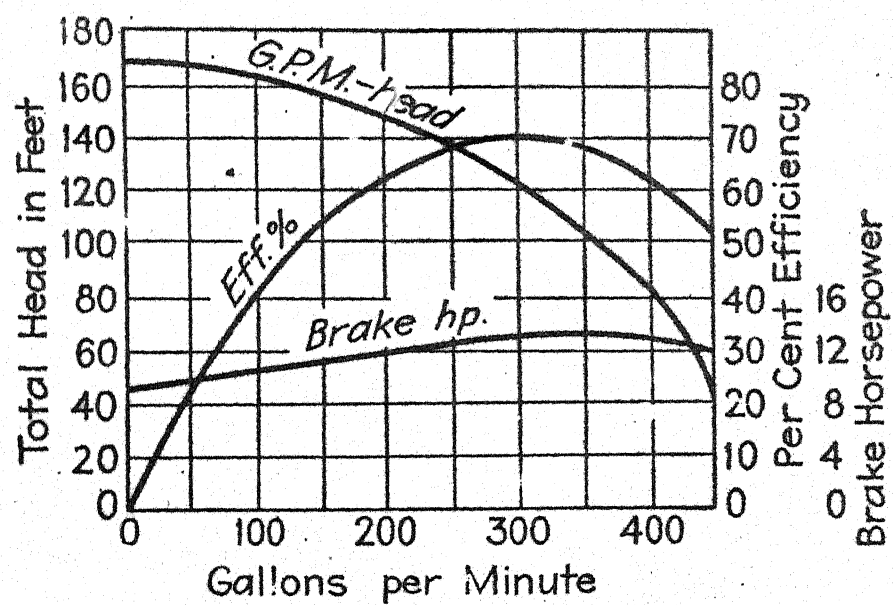
Fig. 2.1(i) Characteristics curves of a centrifugal
pump
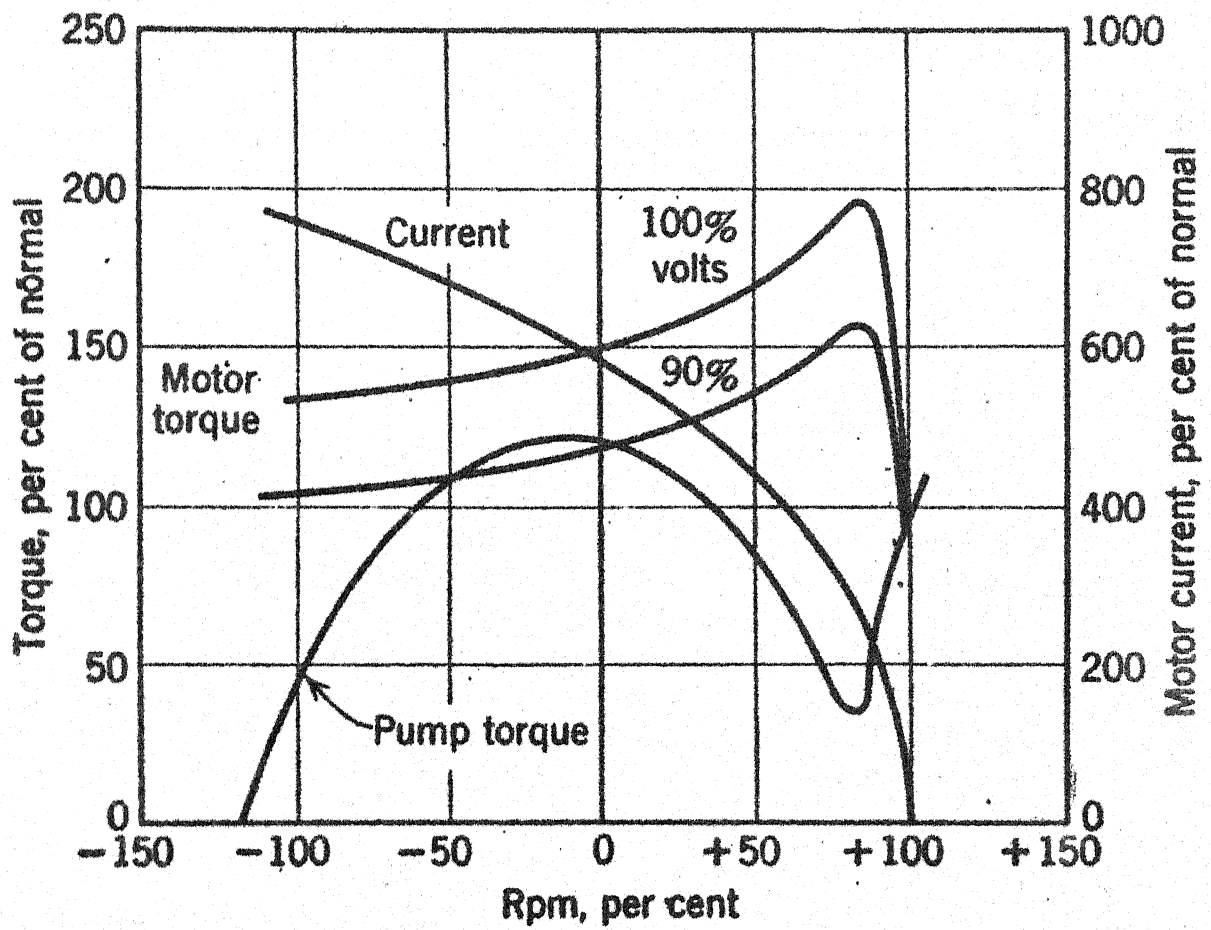
Fig. 2.1(ii) Speed-torque curves: pump n_s = 1800, four pole motor

are compared and the most economical system is chosen.

2.3.1 Solar Powered d.c. Motor

Figure 2.1A shows the schematic diagram of a motor
photovoltaic converter system. The d.c. motor-centrifugal
pump set fed by solar power had been operationally tested and
the performance was reported to be satisfactory (6,7).

In France, a water pump drive powered by solar cells
has been developed (8) . The solar cell array consists
of 56 photovoltaic panels each producing 10.7 V at 25°C.
The optimum operation voltage was found to be 32 V, thus
connecting 2 panels in series and 28 of these in parallel.
The total current delivered is 20A and total power is 500 W.
The low voltage operation has been preferred because a cell
deficiency or a shading effect on a cell has a negligible
effect on the array output. The motor ratings were 32 V,
14 A, 1600 rpm and 500 W.

The main drawback with the d.c. motors is that the
commutator and brushes require frequent maintenance and
replacement. It also requires adequate protection against
the large voltage in the solar cell array, if any. If the
voltage drop in the solar cell array is quite large,
the motor characteristics will suffer and may lead to the
damage of the motor.

2.3.2 Brush and Commutatorless Motor

The d.c. excitation of a synchronous motor is provided by an a.c. exciter and diode bridge. This is shown in Fig. 2.2. The exciter with stationary field and rotating armature is mechanically coupled to the synchronous machine and the diode bridge is placed on the shaft. The connecting leads from the exciter to the diode bridge and then to the field are taken through a hollow shaft. Such a motor is referred to as a brushless d.c. machine. The brushless motor operates the same way as the synchronous motor i.e. it obtains power to its field winding from a direct controlled a.c. exciter and rectifiers (9) .

The advantages of this system are the following :

a) Brushes are totally eliminated thus solving a lot of maintenance problems.

b) A very small excitation is required for the exciter field.

c) Due to the absence of sparking, no costly enclosure is required.

d) The motor speed is constant.

But the main disadvantage of this system is its added cost. It needs a lot of accessories like three phase inverter, diode bridge to be mounted on the shaft, a.c. exciter etc. In addition, a special type of a.c. exciter is needed, whose armature is rotating. Thus, this system is obviously uneconomical and has not been experimented for a solar power drive.

Sun light

SOLAR ARRAY

Static Inverter

D.C. FIELD (STATOR)

Arm. & Rectifiers (Rotor)

D.C. Field (Rotor)

Armature (Stator)

Exciter

Mech. Coupling

SYNC MOTOR

Pump
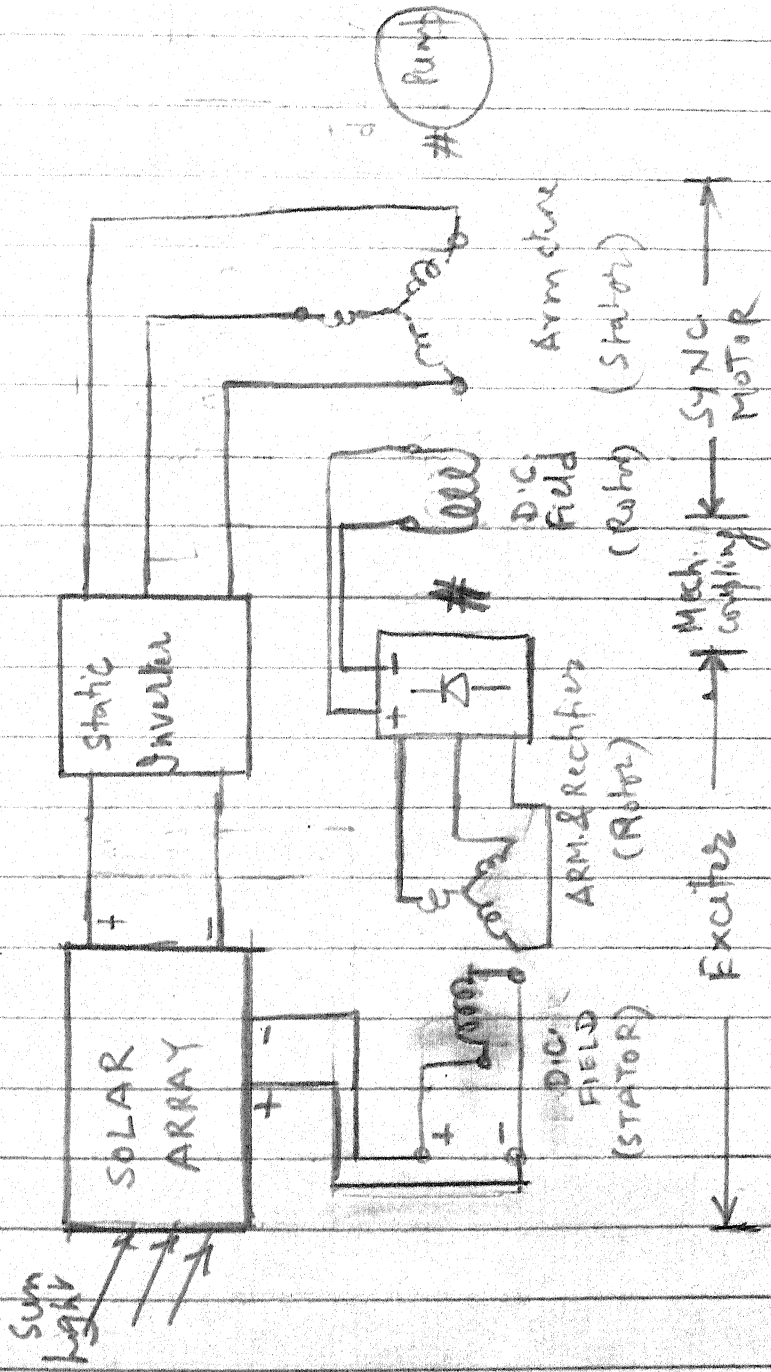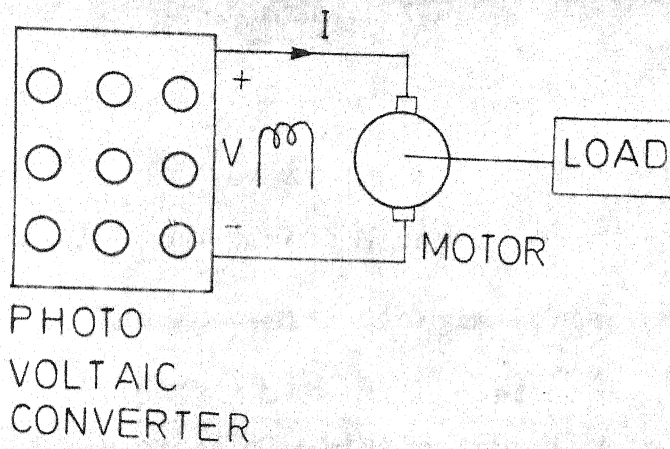
FIG. 2·1A SOLAR POWERED D.C. MOTOR
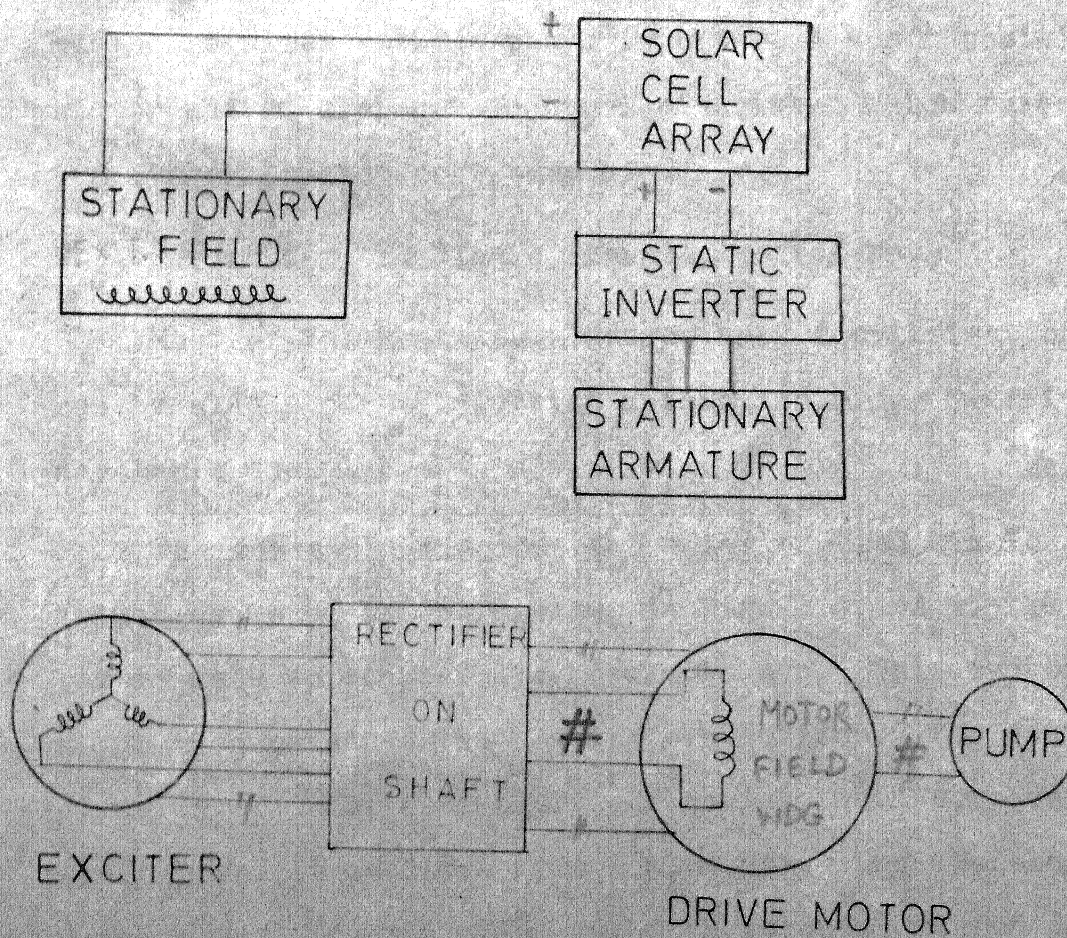
FIG. 2·2 BRUSH AND COMMUTATORLESS MOTOR

2.3.3 Synchronous Motor

The schematic diagram of the solar powered synchronous motor drive is shown in Fig. 2.3. By varying the triggering frequency of the static inverter in conjunction with the shaft position sensor, the speed of the rotating magnetic field can be controlled from zero to the rated value, thus obtaining the characteristics similar to d.c. motor.

But the brushes have not been eliminated here as the solar power is to be fed through it. Another major disadvantage is that the number of components is high, as the system requires a three phase inverter, a shaft position sensor and an elaborate control circuitry which raises the overall system cost very high.

2.3.4 Inverter Fed Single Phase Induction Motor

Most of the centrifugal pumps used for irrigation are run by single phase induction motors, as a.c. power is available cheaply.

The schematic diagram of a solar powered single phase induction motor drive is shown in Fig. 2.4. A static inverter is used to convert d.c. power to a.c. This system is simpler compared to the earlier a.c. drives. The control circuitry is also simpler. Of course, when compared with d.c. drive, it requires more components. But there are other advantages. The induction motor is robust, rugged and
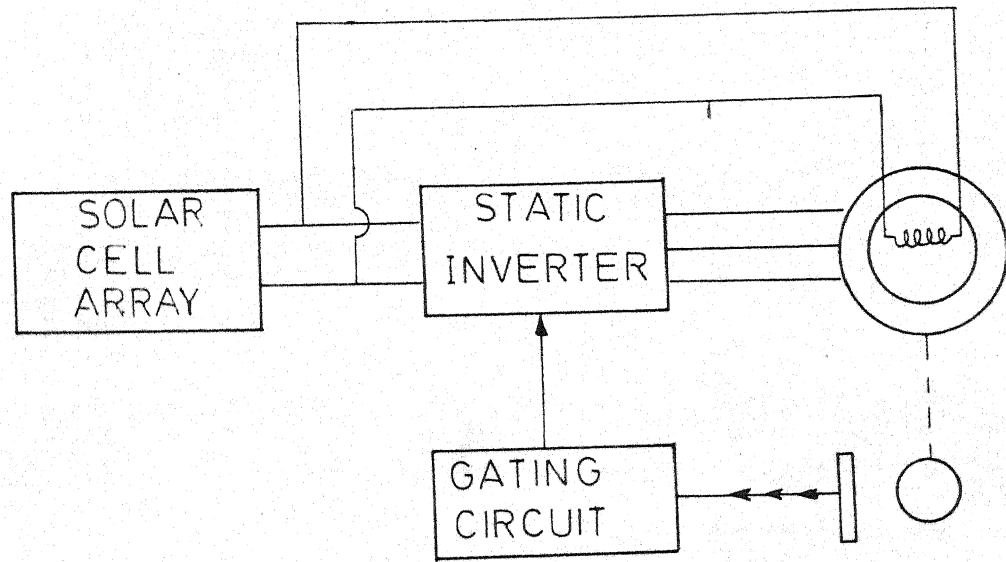
FIG. 2·3 SYNCHRONOUS MOTOR
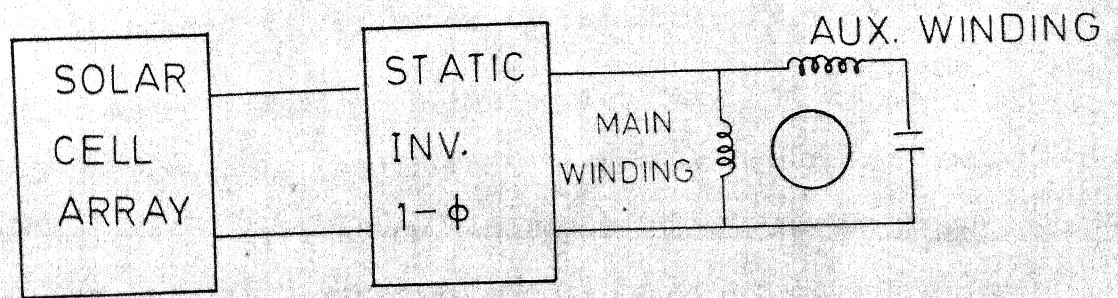
FIG. 2·4 INVERTER FED SINGLE PHASE
INDUCTION MOTOR

maintenance free due to the absence of commutator and brushes. No versatile control characteristics are required for pump applications. Furthermore, no special construction is necessary. Presently such pumps are manufactured by several companies.

2.4 CONCLUSIONS

The ever increasing rate of consumption of the energy available has started the thought 'Is energy inexpendable?'. The answer to this has already arrived through various studies and statistics, that the consumption of fossil fuels at this rate will soon lead to total depletion of them. An alternative source of energy which will be more or less a perpetual source, was found to be the solar energy. Till today, it has indirectly been the source of fossil energy stored in the earth's crust but now solar energy has to be exploited directly.

India's main 'industry' being agriculture, it is expected that solar energy would be utilized to supply power for pumping applications in irrigation, wherever first level ground water is available at low heads. Small plots of land can be easily irrigated using small sized solar powered motor pump set.

Recognizing the source of power in d.c. form, four possible electric drive configurations are presented in this

chapter. Of these four configurations, the solid state single phase induction motor drive seems to be the most economical drive, and also highly reliable and rugged, with minimal maintenance. Such a drive is considered for detailed study and the whole system is described in the next chapter.

CHAPTER 3

SOLID STATE SOLAR POWERED PUMP DRIVE

3.1 INTRODUCTION

In Chapter 2, four possible electrical drive configurations are proposed for a centrifugal pump using solar energy. It is concluded that the single phase induction motor is, by far, the most suitable prime mover based on the following factors :

i)   the single phase induction motor is rugged and robust;

ii) there are no maintenance problems due to the absence of commutator and brushes;

iii) it is economical to use single phase motor;

iv) since no special constructional changes are required, such motors could be easily available at the desirable hp ratings to the consumers by the Indian Industry;

v)   the induction motor is quite suitable for pump applications.

The block diagram of the drive is shown in Fig. 3.1. The solar cells are arranged in several series/parallel combinations to obtain the required voltage and current ratings. Since the power produced by the solar cell array is in dc form, the power modulator should be of necessity a single phase inverter. This inverter converts dc to ac power. The ac power is then fed to the motor-pump set.
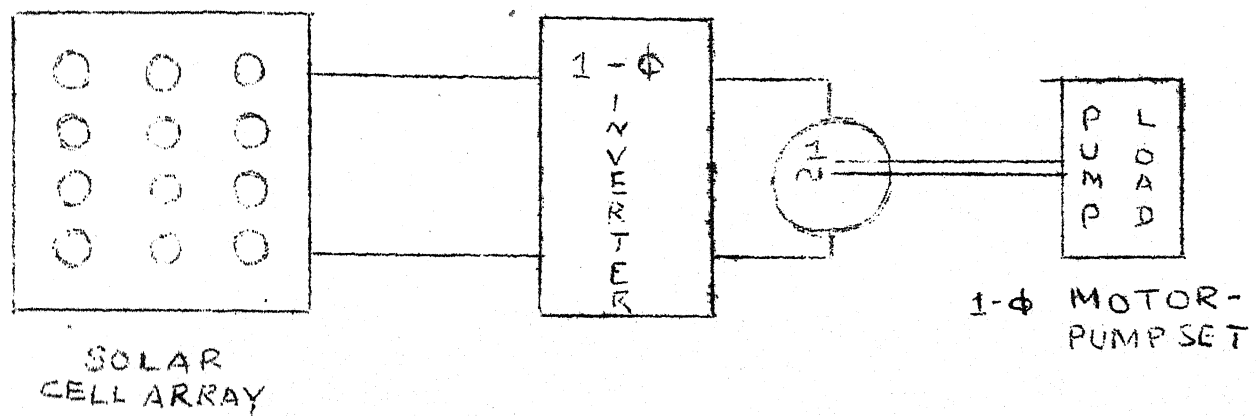
Fig:3.1 BLOCK DIAGRAM FOR SOLAR PUMP DRIVE
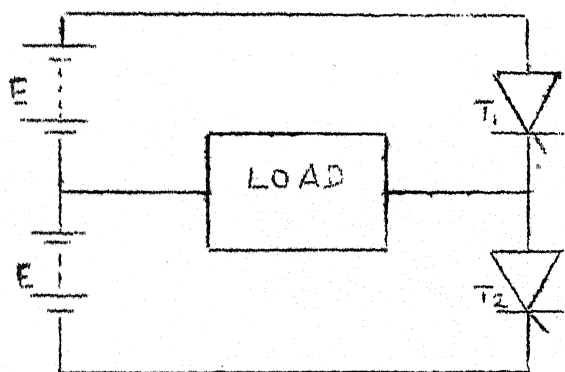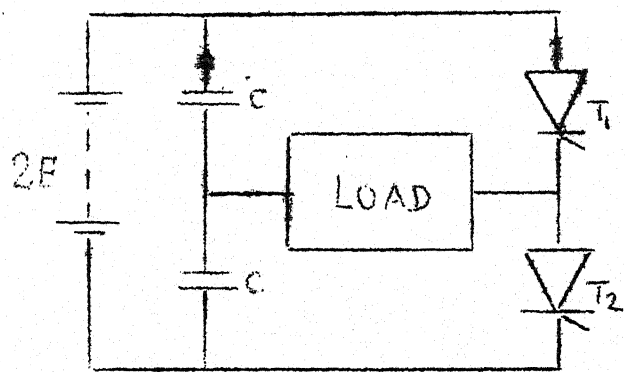
(i)   (ii)

Fig:3.2(a) CENTRE TAPPED SUPPLY
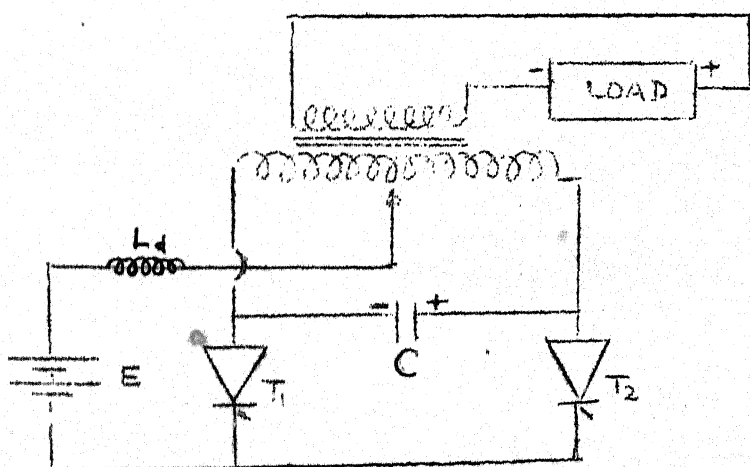
Fig:3.2(b) CENTRE TAPPED LOAD.
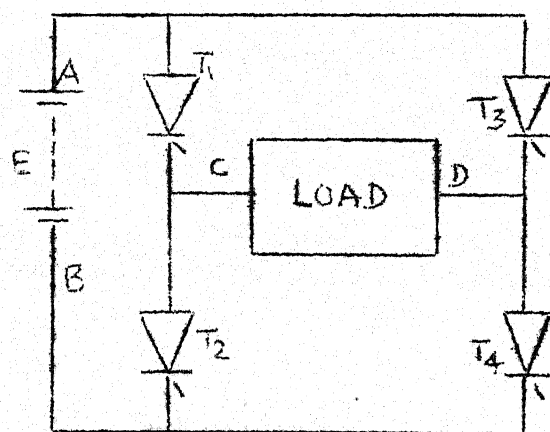
Fig:3.2(c) SINGLE PHASE BRIDGE

The output voltage of a solar cell array is very much dependent upon the brightness of the sun unless some additional storage devices are used. The use of batteries as storage devices is unwarranted because of additional cost and complexity. In order to ensure a constant voltage supply to the motor-pump set throughout the day, when the sun is not bright, a chopper is to be inserted between the solar cell array and the single phase inverter. The function of the chopper is therefore to boost the voltage and supply fairly constant voltage supply to the inverter.

There are many types of inverters and each has its own advantages and disadvantages over the other. In this chapter, a comparative study of different single-phase inverter circuits is presented. The basic principles of choppers are outlined and the working of a step-up chopper is detailed. Finally, the power modulator-chopper and inverter configuration chosen for the detailed study is presented.

3.2   INVERTER CIRCUITS

An inverter converts d.c. power to a.c. power at some desired voltage and frequency. In most modern inverter circuits SCRs are generally used because of their higher efficiency and reliability, fast response, low maintenance, long life, compact size and weight, silent operation etc. The process of turn off of SCRs in inverter circuits is known as commutation. So the basic classification of inverter circuits

is recognised by the different methods of commutation of an
SCR. There are six classes of commutation (10,11) :

Class A : Self commutated by resonating the load

Class B : Self commutated by a LC circuit

Class C : C or LC switched by a load carrying SCR

Class D : C or LC switched by an auxiliary SCR

Class E : External pulse source for commutation

Class F : AC line commutation

Of these six classes, the first five classes (A to E) of
inverters can function independently and provide an ac output
of variable frequency. Such inverters find wide spread appli-
cation in (i) standby power supplies, (ii) UPS in computers,
(iii)speed control of ac motors,(iv) air-craft power supplies,
(v) induction heating, to cite only some areas. The ac line
commutated inverters (Class F) cannot function independently
and provide an ac output of variable frequency. As the name
indicates, the ac voltage is essential for commutation. Basi-
cally, the operation of a line commutated inverter is an
extension of phase controlled rectifier operation, where the
phase angle delay is beyond 90° and the power flow gets
reversed. Such inverters are used in applications such as
i) HVDC systems ii) Regenerative braking of dc drives and
hence their usage is limited. The requirements for the
operation of line commutated inverters are : i) ac source
should be available, ii) the load should consist of a source

of dc power and iii) phase delay has to be more than 90°.

Another way of classifying inverters is based on configuration itself. Based on circuit arrangement, rectifier circuits can be arranged in several configurations such as half-wave, fullwave, bridge etc. Inverter circuits also may be grouped in an analogous manner. The most important configurations are (i) centre-tapped supply, (ii) centre tapped load, (iii) single phase bridge, and (iv) three phase bridge, as shown in Fig. 3.2. Each inverter configuration can be built by any one of the commutations listed above. As a result, several inverter circuits can be developed.

In solar powered pumping applications, the main source of input power to the drive system is dc. Obviously an inverter circuit based on forced commutation is to be selected to run the single phase induction motor. The inverter chosen should be simple, economical and provide good performance. Before we take up single-phase inverter circuits, let us look into the basic requirements of a forced commutated inverters.

A basic bridge inverter is shown in Fig. 3.2(c). The operation of the circuit is as follows : SCRs T_1 and T_4 are triggered to cause the current to flow through the load from C to D. After half the period of output frequency, T_1 and T_4 are commutated and T_2 and T_3 are triggered. This causes the current to flow from D to C. After half the period, T_2 and T_3 are commutated and the cycle continues.

In this type of inverter, T_2 is triggered immediately after commutation of T_1. Thus the triggering of T_2 will make point C to attain the potential of point B, which forward biases T_1. Therefore, T_2 is triggered after sufficient delay, so that T_1 is reverse biased for sufficient time. In inverter circuits, retriggering or spurious triggering of a commutated device would certainly result in a short circuit. If, in Fig. 3.2(c) T_1 and T_4 are conducting and if for any reason T_2 gets triggered, it is seen that a dead short circuit across the d.c. supply would take place. Therefore, in addition to using special inverter grade thyristors, we should take all precautions to prevent spurious pulses. The devices used in inverters should be capable of (i) blocking the forward voltage, (ii) quick turn off and (iii) withstanding large dV/dt (10,12).

As each SCR requires a separate commutation circuit, the number of components increase. Thus the overall cost of the inverter increases, which makes it economically incompetitive.

The other simple single-phase inverters are (a) series inverter (b) parallel inverter which are described in the following sections.

(a) Series Inverter :

Series inverters are commonly used when a high output frequency of some 200 Hz to 100 KHz is required. Such high

frequencies may be desirable in induction heating, flourescent lighting etc. Series inverters operate on load commutation (Class A). L-C components are added to the load circuit. They are particularly suitable for high frequency operation since the size of L-C components decreases with an increase in frequency. A basic series inverter is shown in Fig. 3.3.

The series inverter cannot operate on no-load and protection against short circuit of the output demands special control features to detect excessive output current or capacitor voltage. The limitations of series inverters are :

i) Its maximum possible output frequency is limited to the ringing frequency of the resonant circuit. This is because SCR2 can be triggered only after SCR1 is put off. Of course, this can be overcome by using a coupled inductor.

ii) For output frequencies much lower than the ringing frequency, the distortion in the load voltage waveform is high because the on-time is quite large in comparison with the duration of conduction of the SCRs.

iii) High rating of the commutating components is required because these components carry the load current continuously and the capacitor supplies the load current in every alternate half cycle.
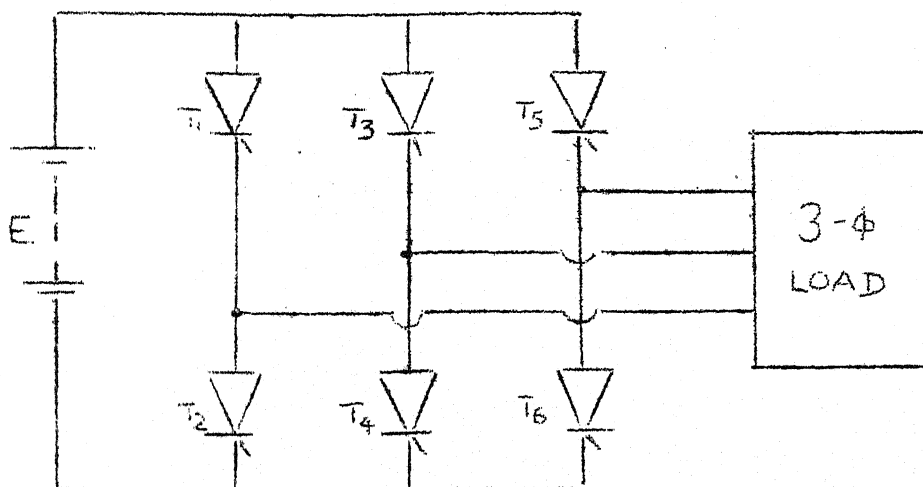
Fig. 3.2 (d) THREE PHASE BRIDGE
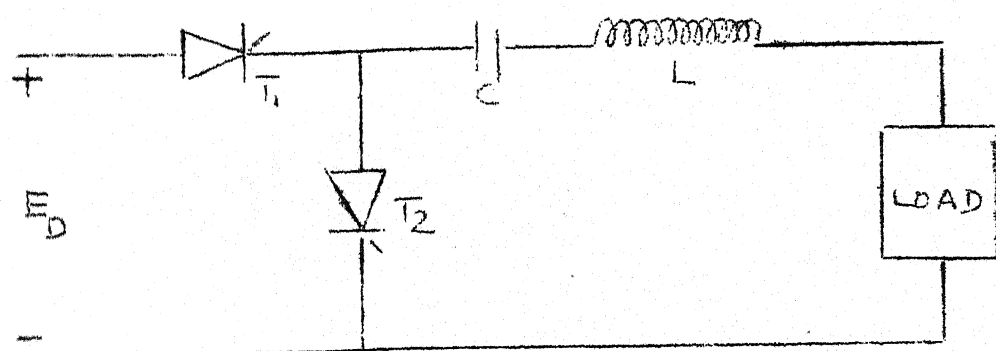
Fig. 3.3 SERIES INVERTER
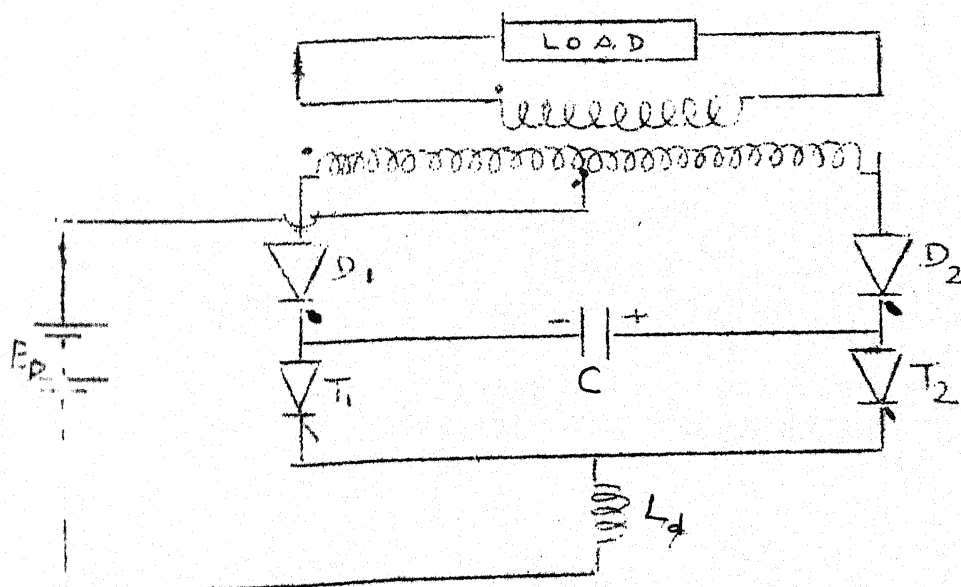
Fig. 3.4 MODIFIED PARALLEL INVERTER

iv) As the power flow from the d.c. source is intermittent, the source should have a large peak current rating and the input current will have a high harmonic content (11).

In pumping applications, the driving motor is to be rated at normal power frequency from viewpoint of economy and other considerations. The inverter, therefore, operates at normal power frequency and large sized commutating components are required. Furthermore, the peak source current might result in substantial drop in the output voltage of the solar cell array.

(b) Parallel Inverter

The basic circuit of this inverter is shown in Fig. 3.2(b) which is a centre tapped load configuration. The capacitor C, effectively in parallel with the load, is providing commutation, while inductance L_d smooths the dc current drawn from the source. The working of the circuit is as follows : Initially T_1 is conducting, then the left half of the transformer primary and L_d gets the supply voltage E_d and the capacitance gets charged to roughly $2E_d$ with the polarity indicated in the Fig. 3.2(b). The load will also have the same voltage transformed and the polarity as shown. Now T_2 is triggered and the capacitor immediately applies its voltage to T_1 through T_2, which reverse biases T_1 and commutates it. With T_2 on, the source voltage will be

applied to the right half of the transformer and the load voltage will also reverse. Thus an alternating voltage and current is obtained in the load.

The output frequency is decided by the triggering frequency of the SCRs. For variable frequency operation, the transformer has to be designed suitably. Two causes of failure of this circuit could be (a) not enough turn off time for the SCR is given which will lead to both the SCRs conducting and a short circuit will result. This can be prevented by increasing the commutating capacitance suitably, (b) Due to large voltage across the SCRs which leads to reverse breakdown. This can be prevented by decreasing commutating capacitance. Therefore, for satisfactory operation of the circuit, a compromise between these two conflicting requirements is to be made.

From the study of different single phase inverters, the parallel inverter appears to be a good choice. The parallel inverter is slightly modified by connecting diodes in series with the thyristors as shown in Fig. 3.4(13,14). The function of these diodes is to trap the charge on the commutating capacitor enabling operations with an ac load of any power factor. In the basic inverter, the commutating capacitor is effectively connected across the load. A part of the commutating energy stored in the capacitor is diverted to the load. Large capacitors are required to handle inductive and back EMF

loads. This is quite pronounced particularly at low frequencies. By connecting these series diodes, the size of the capacitor can be reduced.

Two broad classes of inverters emerged over a period of last one decade. They are (i) Voltage Source Inverters (VSI) (ii) Current Source Inverters (CSI). Voltage source presents a low impedance while current source presents high impedance to the inverter. Current source inverters are becoming popular for ac motor drives, induction heating and a variety of inverter applications. Any commutation failure in VSI may result in a large short circuit current. This may damage the device and other circuit components. The main advantages and disadvantages of CSI are :

i) Inverter grade thyristors with low turn off time, which are costly, need not be used.

ii) Inherently protected against short circuit at the output terminals.

iii) Reliability and ease of regeneration when fed through a phase controlled rectifier.

iv) Simpler and more rugged.

v) Open circuit at the output causes very high voltages.

vi) Main limitations are weight, volume, cost and load dependence.

In the present study, the CSI is preferred over the VSI because of the several advantages mentioned above. It may,

however, result in some extra cost. The parallel inverter with the series diodes is provided with a large inductor in its front end so that the voltage source may be converted into a ripple free current source. Fig. 3.4 shows this modified parallel inverter. The operation of the inverter can be described as follows :

Due to the continuity of the direct current fed through the inductor L_d, atleast one of the thyristors T_1 or T_2 is forced to conduct. However, due to capacitance C, only one can conduct at a time. This is because, if T_1 is conducting and the capacitor is charged as shown, then T_2 cannot be turned on as it is reverse biased. After the capacitor gets charged in the reverse direction, T_2 can be turned on, but the capacitor voltage reverse biases T_1 and turns it off. Even if the capacitor voltage is zero when both T_1 and T_2 are gated on, the action of the counter emf will extinguish the current in one of the thyristors and then charge the capacitor(14).

When T_1 conducts, either D_1 or D_2 or both of them can conduct depending on the capacitor voltage and the counter emf. Similarly with T_2, these modes can take place. The analysis during different modes is taken up in the next chapter.

The whole system block diagram is shown in Fig. 3.1.
It consists of (i) dc source from solar cell array, (ii)
current source modified parallel inverter, and (iii) single-
phase induction motor-pump set. The system may operate
satisfactorily during the day time when the sun is bright.
Due to the inherent intermittent nature of solar energy, the
input source may not provide a constant voltage supply. In
order to maintain a constant voltage/current to the inverter
under all weather conditions, a step up chopper is inserted
between power source and the inverter. The function of
this chopper is to develop a constant voltage/current for the
inverter. V-I curves of solar cell is shown in Fig. 3.4A.

3.3 CHOPPER

A chopper circuit converts d.c. power from a constant
voltage (input) to a variable voltage (output). The chopper
circuits, depending upon the operation in the V-I plane (in-
stantaneous values), are classified one-quadrant, two-qua-
drant, four quadrant configurations. Choppers are widely
used in d.c. motor control, battery charging, regulated
power supplies, battery operated vehicles etc. The SCR
choppers offer greater efficiency, faster response, lower
maintenance, smaller size than motor-generator sets.

A basic single quadrant chopper is shown in Fig. 3.5(a)
(15). The dotted box indicates SCR chopper consisting of
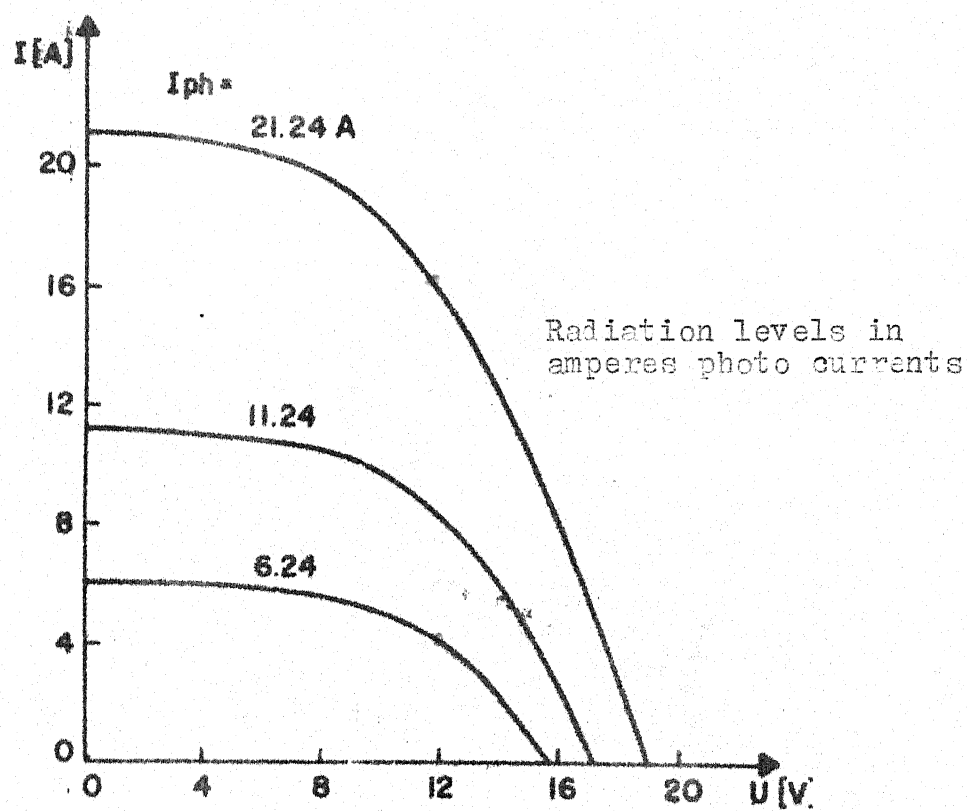main SCR and its commutating circuitry. It may be considered

Fig. 3.4A V-I characteristics of solar cell
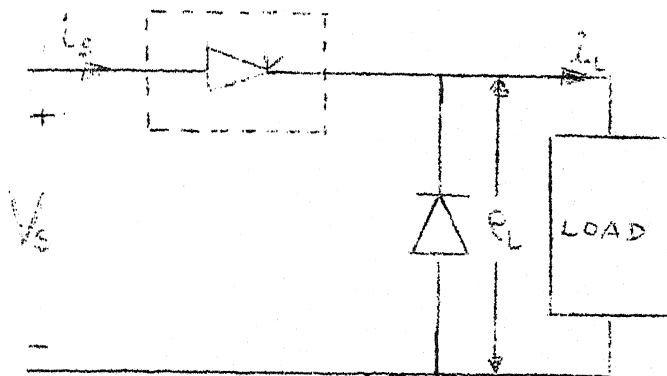
Fig. 3·5(a) BASIC CHOPPER
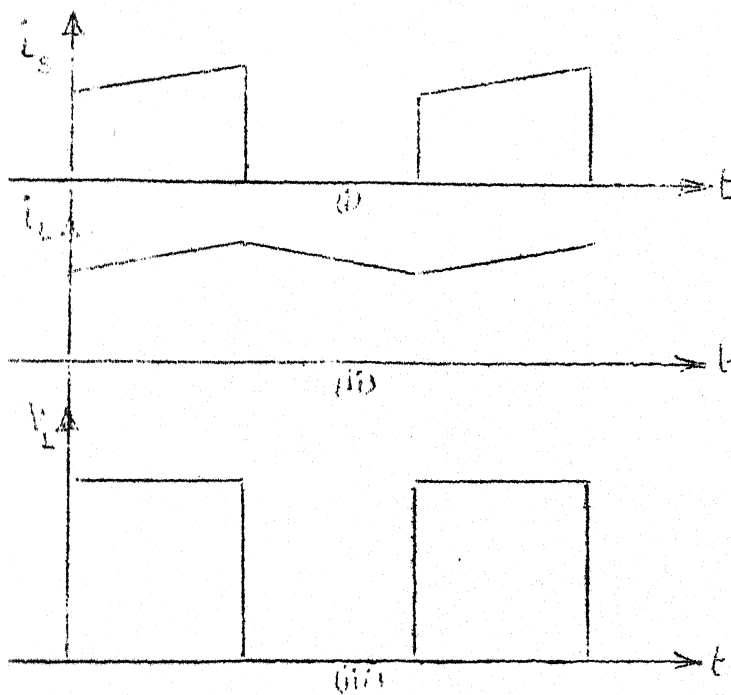
(i) SOURCE CURRENT

(ii) LOAD CURRENT

(iii) LOAD VOLTAGE

Fig. 3·5(b) WAVE FORMS OF VOLTAGE & CURRENT

to be an ideal switch. Assuming continuous current, the output voltage is completely defined as follows :

$$V_L = V_S \text{ , when chopper is on}$$

$$V_L = 0 \text{ , when chopper is off}$$

By operating the chopper periodically, a rectangular train of pulses e_L as shown in Fig. 3.5(b) can be generated. The average value of the output voltage, v_L is given by,

$$V_L = V_S \cdot \frac{t_{ON}}{T}$$

Thus the average voltage can be varied from 0 to V_S by the following control strategies :

i)   Constant frequency, variable ON time

ii) Variable frequency, constant ON time

iii) Variable frequency, constant OFF time.

The output voltage waveforms using these control strategies are illustrated in Fig. 3.6 (16).

With the chopper described above, we can obtain an output voltage which is less than or equal to the input voltage. This type of chopper is called step down chopper. There are other types of choppers,

i)   Step-down and boost and, ii) Step-up chopper,

i) Step-down and boost chopper :   Fig. 3.7 shows the simplified circuit configuration for a step-down and boost chopper.
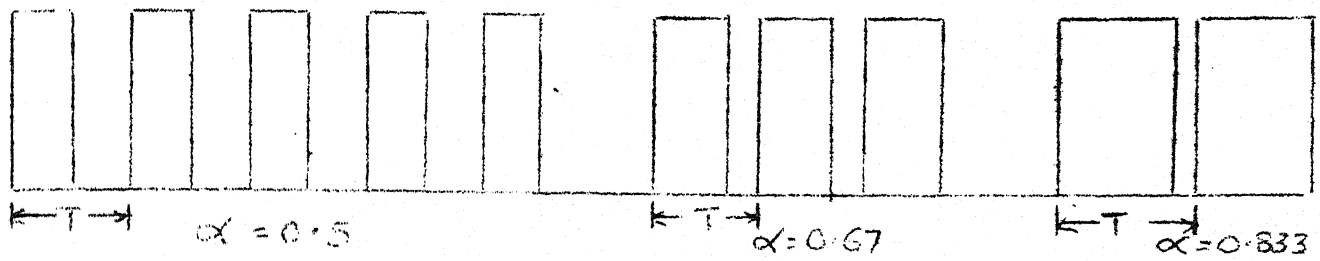
(a)
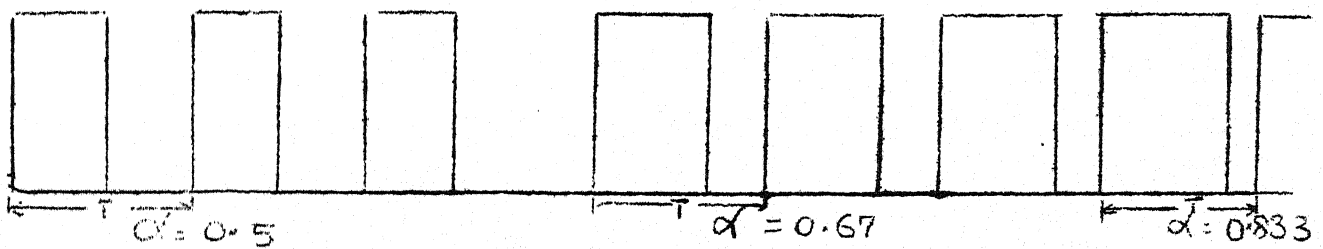
(b)
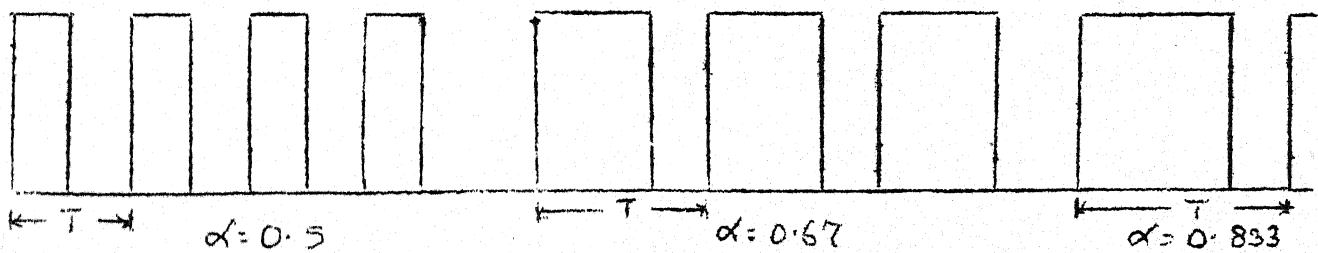
(c)

Fig 3.6   CHOPPER CONTROL STRATEGIES

(a) Constant Frequency T_{RC}

(b) Variable Frequency – constant-on-time

(c) Variable Frequency – constant off-time

When switch S is closed the source voltage V_S is impressed across the inductor L. When S is opened the inductor voltage, $L \frac{di_1}{dt}$ must equal V_L, and the energy stored in the inductor is transferred through the diode into the battery. The source voltage V_S is unconstrained and can be greater or less than V_L.

The current flows through the inductor continuously, whether or not the switch S is open or closed. Thus neglecting ripple, $I_1 = I_2 =$ constant and

$$V_S \, I_1 \, t_{ON} = V_L \, I_1 \, t_{OFF}$$

$$\frac{V_L}{V_S} = \frac{t_{ON}}{t_{OFF}} = \frac{t_{ON}}{T - t_{ON}} = \frac{\delta}{(1-\delta)}$$

where

$$T = t_{ON} + t_{OFF} = \text{chopper period}$$

$$\delta = t_{ON}/T$$

As δ increases from 0 to 0.5, the load voltage increases from zero output voltage to source voltage and for δ greater than 0.5, the load voltage is greater than the source voltage.

(ii) Step up chopper : Fig. 3.8 shows the circuit configuration for a step up chopper.

When the switch S is closed, energy is stored in the inductor . When the switch opens, the sum of $L \frac{di}{dt}$ and source voltage are impressed across the load. The energy stored in the inductor is transfered to the load and also charges up the capacitor C. The capacitor C maintains the output voltage constant when the switch is closed. Assuming that the current through the inductor is continuous,

$$V_s \, I_1 \, T = V_L \, I_1 \, t_{off}$$

$$\frac{V_L}{V_s} = \frac{T}{t_{off}} = \frac{T}{T - t_{ON}} = \frac{1}{1 - \delta}$$

As δ increases, the output voltage increases above that of the source voltage, thus stepping up the voltage.

3.4 STEP UP CHOPPER INCLUDING COMMUTATION CIRCUIT

The complete chopper circuit used is shown in Fig. 3.9. The thyristor T_{M1} acts as the main switch and the commutation circuit consists of a capacitor C_c, auxiliary thyristor T_c, inductor L_c and recharging thyristor T_{M2}. The following assumptions are made in the operation of the chopper :

a)   The inductance L_1 is so large that the current ripple is negligibly small.

b)   The capacitor C is large enough to keep the load voltage V_L constant during the chopper off period.

With these assumptions, the circuit operation may be described as given below.
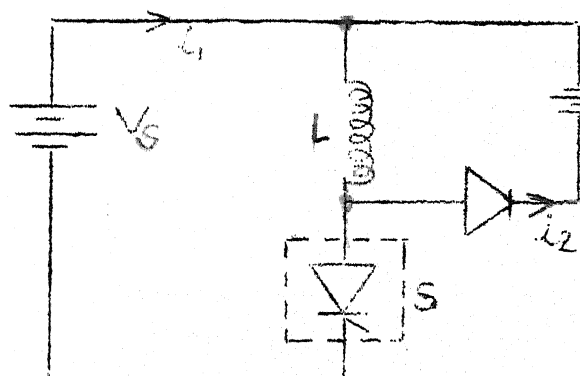
Fig. 3.7. STEP DOWN AND
BOOST CHOPPER
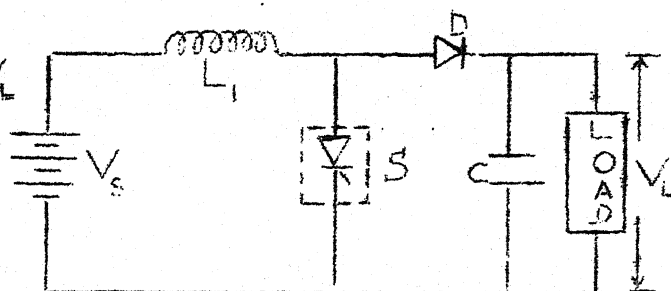
Fig. 3.8 STEP UP CHOPPER
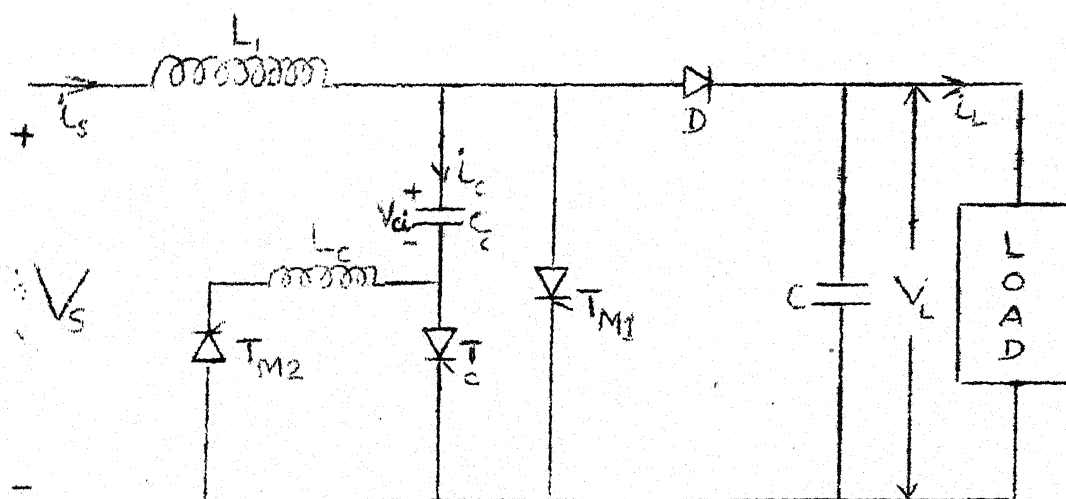
Fig. 3.9 COMPLETE CHOPPER CIRCUIT

Interval I : The commutating capacitor C_c is charged to an initial value from an earlier operation. When the thyristors T_{M1} and T_{M2} are triggered, the source current flows through the inductor L_1 and T_{M1}. At the same time, the voltage across the capacitor C_c reverses through T_{M1}, T_{M2}, inductor L_c and C_c. The current in this loop has oscillating response. The current increases sinusoidally and decreases to zero. As the current i_c tends to reverse, the thyristor T_{M2} turns off. The interval I ends when the current, i_c becomes zero. The equivalent circuit for this interval is shown in Fig. 3.10(a).

The equation for the loop formed by source, inductance L_1 and T_{M1} is given by

$$V_s = L_1 \frac{d\,is}{dt} \qquad (3.1)$$

Hence

$$i_s = \frac{V_s}{L_1} t \quad (0 < t < \pi \sqrt{L_c C_c})$$

Considering the other loop formed by capacitor C_c, T_{M1}, T_{M2} and inductor L_c, and with an initial voltage v_{ci} across capacitance C_c, the equation for this is

$$L_i \frac{di_o}{dt} + \frac{1}{C_c} \int_0^{t_{ON}} i_c \, dt + v_{ci} = 0 \qquad (3.2)$$

Solving for i_c with initial conditions $i_c(o) = 0$, $\frac{di_c}{dt}(o) = -\frac{v_{ci}}{L_c}$, we get

$$i_c = \frac{-v_{c_i}}{L_c} \sin \omega t$$

where

$$\omega = \frac{1}{\sqrt{L_c C_c}}$$

Therefore, from the above equations the voltage across the capacitor is given by

$$V_c = v_{ci} \cos \omega t$$

At $\omega t = \pi$, the current i_c is zero and the thyristor T_{M2} turns off. At this time, the voltage across capacitor V_c equals to $- v_{ci}$ which is got from the above expression for v_c by substituting $\omega t = \pi$. The time variations of waveforms of v_c, i_s, V_L and i_c are illustrated in Fig. 3.11(a).

Interval II : The circuit for this interval is shown in Fig. 3.10(b). Only thyristor T_{M1} is conducting and the voltage equation of this loop is the same as equation (3.1). The initial condition is

$$i_s(o) = I_1 \pi \sqrt{L_c C_o}$$

The waveforms pertaining to this interval are given in Fig. 3.11(a). This interval lasts for $(t_{on} - \pi \sqrt{L_c C_o})$.

Interval III : The voltage across the commutating capacitor is of right polarity to commutate. This interval is shown in Fig. 3.10(c). At the end of the ON period, T_{M1} is to be

commutated. To commutate T_{M1}, auxiliary thyristor T_c is triggered. The voltage across C_o is applied across T_{M1} which reverse biases it and T_{M1} turns off. The capacitor C_c gets charged through the source and as soon as it is equal to the load voltage, the diode D conducts. Thus the voltage across C_c is clamped to the load voltage.

During the commutation interval which is very small, the current through the inductor L_1 is assumed to be constant. Therefore, when T_c is triggered to commutate T_{M1}, the capacitor C_c charges linearly by constant current (I_{L1}).

The loop formed by source, inductor L_1 and commutating capacitance C_c can be mathematically represented by

$$V_s = \frac{1}{C_c} \int_0^{t_2} I_{L_1} dt - V_{ci} \qquad (3.3)$$

Here the drop across the inductance L_1 is zero and the current I_{L_1} is constant. But at $t = t_2$, voltage across capacitor equals load voltage and D_2 starts conducting. Therefore,

$V_c(t = t_2) = V_L.$

Interval IV : The capacitor C gets charged to the sum of the source voltage and $L \frac{di_s}{dt}$ which is the load voltage. Considering the operating circuit for the interval (Fig. 3.10(d)),

$$V_L = V_s + L_1 \frac{di_s}{dt} \qquad (3.4)$$

The waveforms corresponding to this intervals are shown in Fig. 3.11 (a) and oscillographs are shown in Fig. 3.11(b).

(a) Interval I   (b) Interval II   (c) Interval III
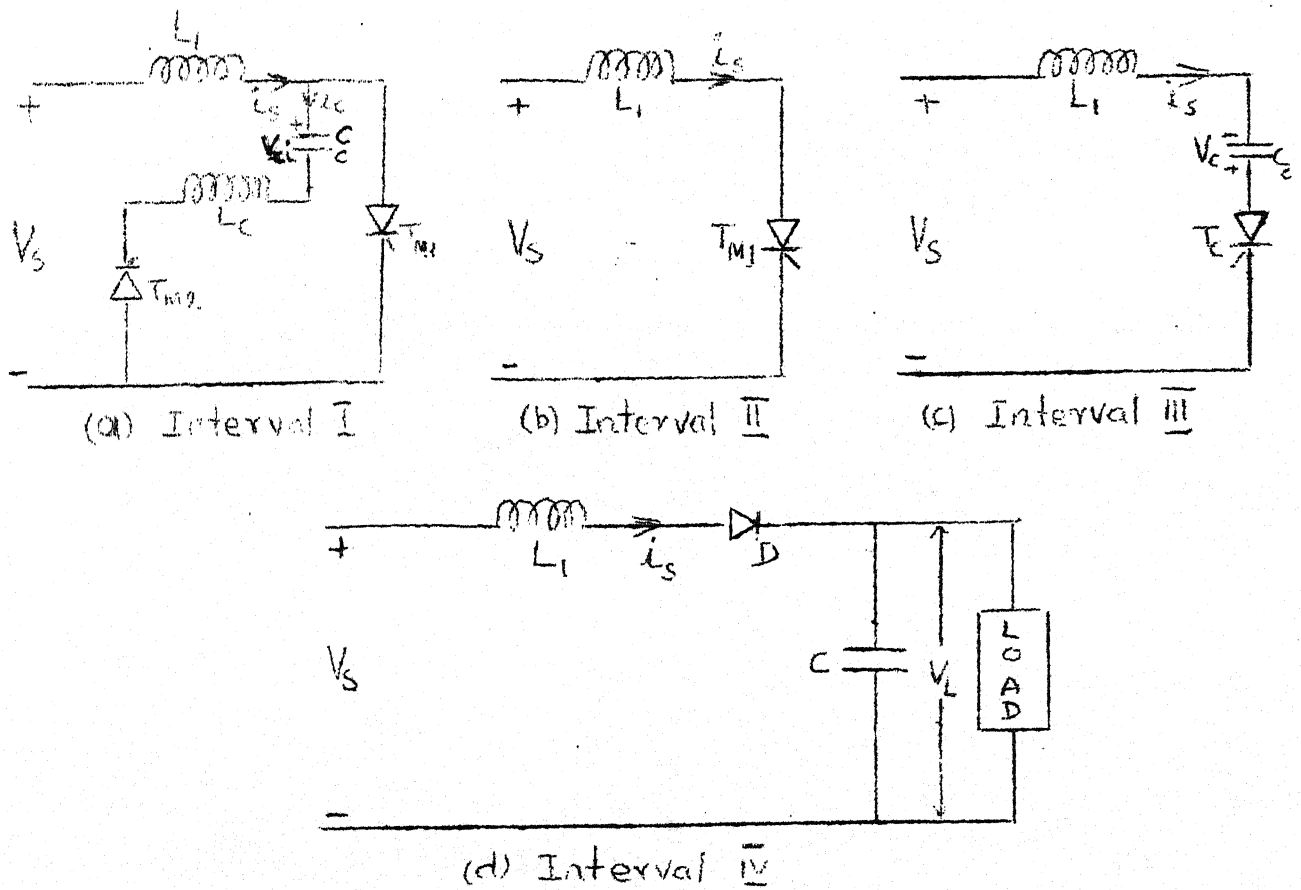
(d) Interval IV

Fig 3.10. DIFFERENT INTERVALS OF CHOPPER
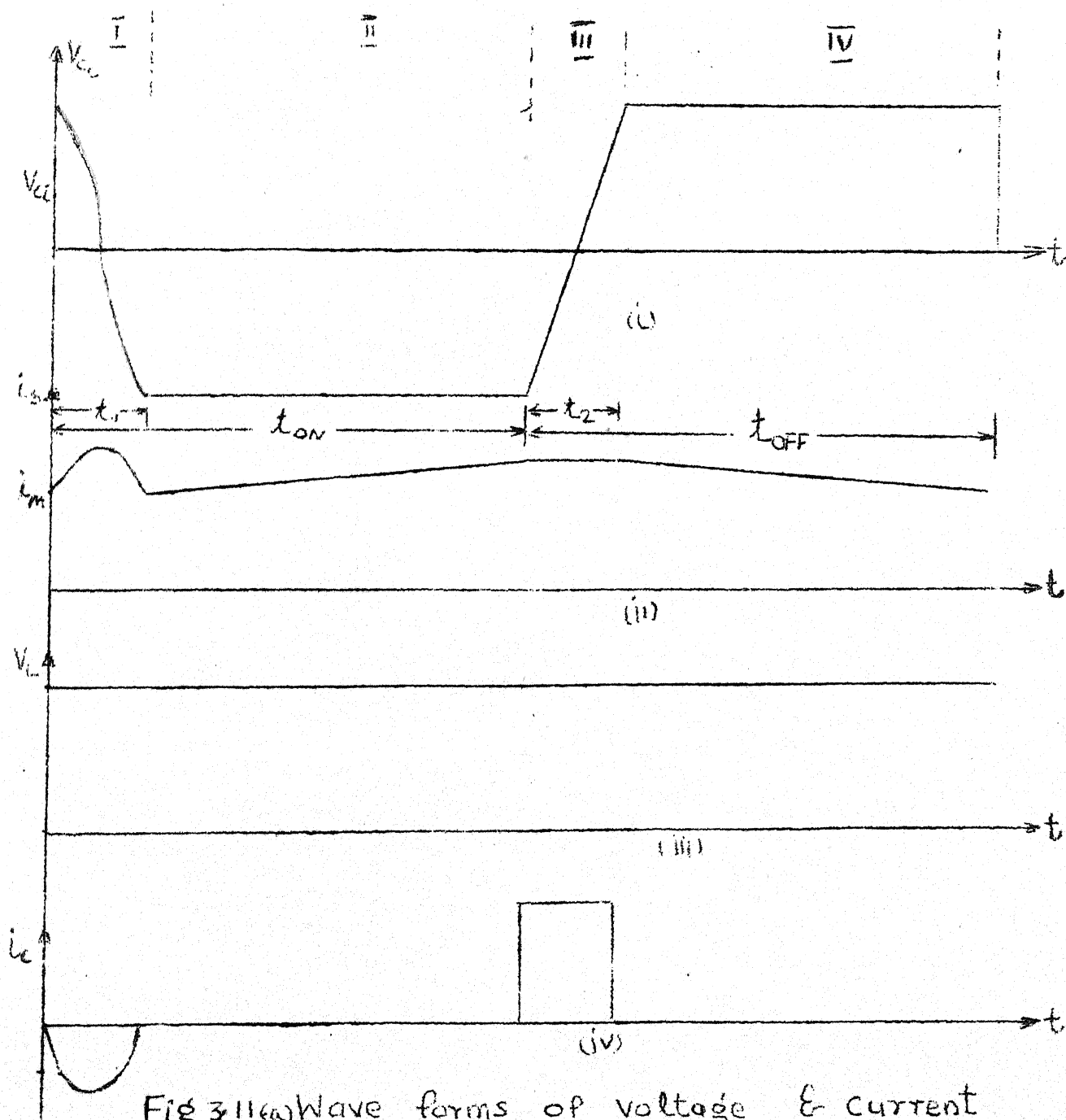
Fig 3 11(a) Wave forms of voltage & current

(i) Voltage across commutating capacitor C_c
(ii) Source current   (iii) Load voltage
(iv) Current through commutating capacitor C_c
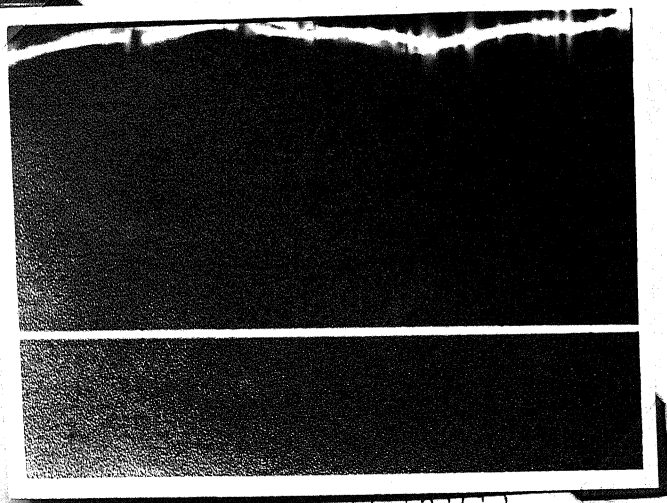
Fig. 3.11 (b)(i)

Source current i_s
Scale: X-Axis- 1 msec/cm
       Y-Axis- 10 mV/cm

Fig. 3.11 (b) (ii)
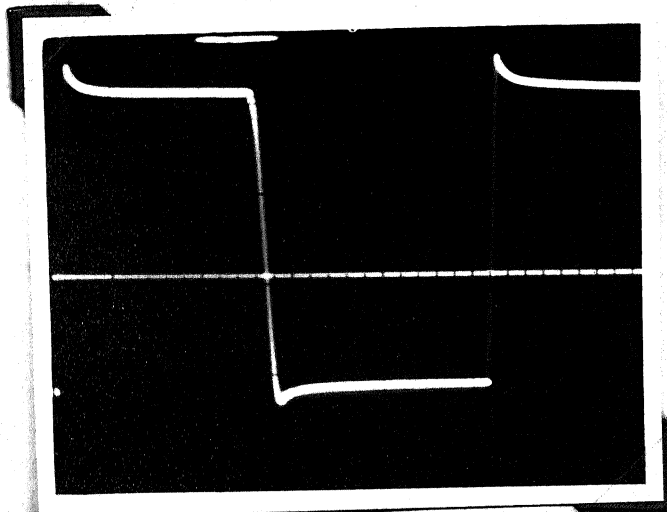
Voltage across commutating
capacitor C_c
Scale: X-Axis - 1 msec/cm
       Y-Axis - 20 V/cm

Fig. 3.11 (b) (iii)

(i) Voltage across main SCR T_{M1}
(ii)Chopper output voltage
     Scale: X-Axis - 1 msec/cm
            Y-Axis - 20 V/cm .

As seen with the ideal case of a step-up chopper, when δ increases, the output voltage should increase indefinitely. The assumptions made regarding the inductor current and the output voltage to be constant is not true in actual working. For long duty interval of the thyristor T_{M1}, the capacitor C acts as the source for the load and in this process, losses some change. During the off time of the thyristor T_{M1}, the capacitor C gets charged but the off time being small, it will not be able to get fully charged. As this cycle continues, the capacitor settles down to a lower voltage. Therefore, in practice, it is not possible to get very large output voltage with a small input voltage.

3.5   OVERALL CIRCUIT CONFIGURATION

The complete circuit diagram consisting chopper and inverter is shown in Fig. 3.12. Some precautions are to be taken for the successful operation of the whole circuit.

a)   Triggering pulses are to be given simultaneously to the chopper and the inverter. If pulses are given first to the chopper, the output voltage may be too small for the load and commutation failure in the chopper may take place.

b)   For smooth starting of the motor and to restrict the in rush current, the chopper output voltage is gradually increased to the rated value. This prevents the sudden application of large voltage across the thyristors.
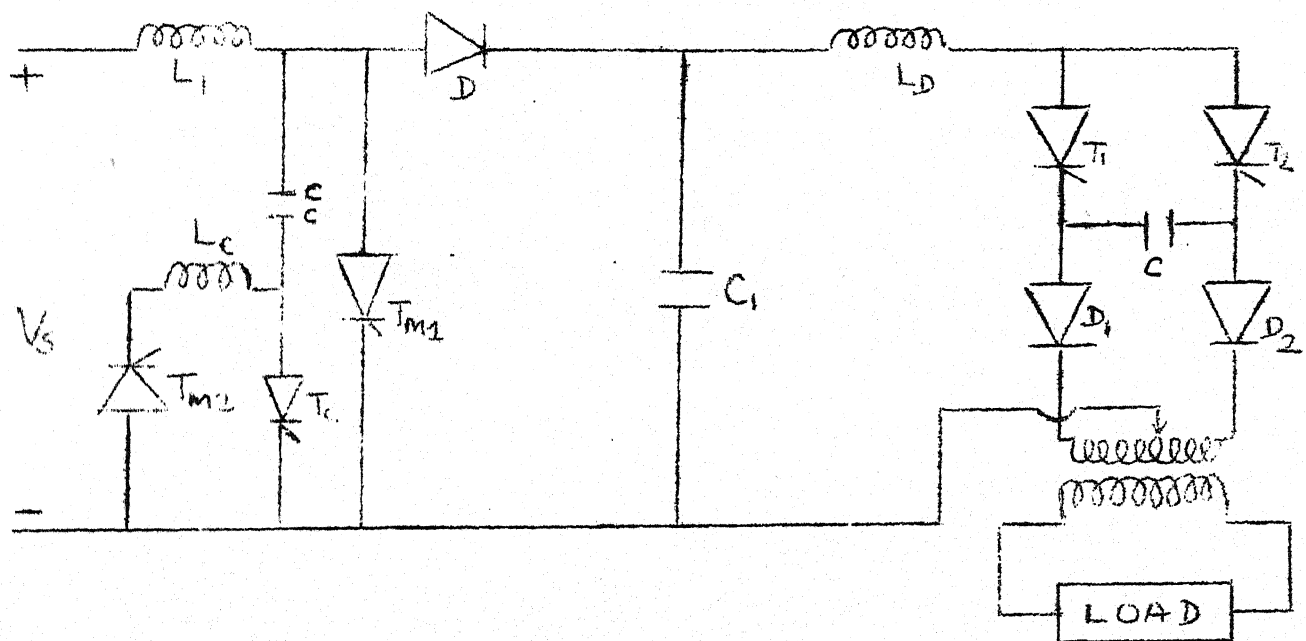
Fig 3.12 OVERALL CIRCUIT DIAGRAM
(CHOPPER & INVERTER)

For loading purposes, a d.c. shunt motor is coupled to
the induction motor. Due to non-availability of centrifugal
pump in the lab the actual motor-pump set could not be
tested. The source for the system, which was proposed to
be a solar cell array, could not be obtained. Therefore,
an MG set was used as the d.c. source to the inverter.

3.6 CONCLUSIONS

A comparative study of different single phase inver-
ters is made. An economical inverter-modified parallel
inverter is chosen for converting d.c. to a.c. in order to
power the motor-pump set. The CSI is preferred to VSI be-
cause of several advantages of the former if a slight in-
crease in cost is tolerated. The voltage output of the
solar cell array is a strong function of solar radiation.
To ensure fairly constant voltage/current input to the
inverter under all radiation levels, a step-up chopper is
to be connected between the source and the inverter. The
step up chopper configuration including effects of commuta-
tion is presented and its operation is described in detail
illustrating the pertinent waveforms.

As a centrifugal pump could not be obtained, the motor
pump set could not be put to actual field test. All load
tests were conducted on the d.c. shunt motor which was cou-
pled to the induction motor. Solar cell array, due to its
non-availability, could not be used to power the system. The

d.c. source was made available through a motor-generator set.

For successful operation of the complete circuit (chopper and inverter) as described in this chapter, the firing pulses have to be given to the thyristors in a particular sequence. The study regarding generation of the firing pulses and other aspects of the control circuit is the subject of the next chapter.

CHAPTER 4

DETAILS OF CONTROL CIRCUIT FOR THE CHOPPER-
INVERTER

4.1 INTRODUCTION

A study of different types of inverters was made and the
modified parallel inverter was chosen to drive an induction
motor-pump set. The parallel inverter chosen has two thyri-
stors which have to be triggered at regular intervals to give
an a.c. output. This interval determines the output frequency
of the inverter. The single-phase induction motors which
are manufactured in bulk, are rated at normal power frequency
of 50 Hz. Thus, by choosing the inverter frequency as 50 Hz,
the normal induction motors which are available can be
directly used and the need for special purpose motors can be
avoided. The other advantage is that the same motor can also
be operated with the normal a.c. supply. The triggering
frequency of the thyristors in the parallel inverter is
designed for 50 Hz. The design of the triggering circuit is
discussed in this chapter.

The d.c. supply is supposed to be obtained from a solar
cell array. This voltage is, therefore, dependent on the
brightness of the sun, which is intermittent. This may cause
the voltage to drop, under some situations thereby affecting

the performance of the motor-pump set. For maximum output from the motor-pump set, the voltage applied across the motor must be held constant. The step-up chopper as proposed earlier ensures steady voltage under all radiation levels. The step-up chopper is operated at constant frequency with variable on-time. The design of the triggering circuit for obtaining the required pulses to the thyristors is discussed in this chapter. The triggering circuit also ensures firing the thyristors in a particular sequence while starting the chopper.

4.2 TRIGGERING CIRCUIT FOR THE INVERTER

The main block diagram for the firing circuit for the inverter is shown in the Fig. 4.1(a) which gives the triggering pulses to the thyristors T_1 and T_2 shown in Fig. 3.4. The waveforms are shown in Fig. 4.1(b). The astable multivibrator produces a sqare wave Ⓐ of the set frequency. This square wave Ⓐ is inverted to obtain Ⓑ. Ⓐ and Ⓑ are then ANDed with a high frequency modulating signal Ⓒ. These two signals with 180° phase shift at the set frequency are applied to the gates of the thyristors through a pulse driver and pulse transformer. The associated circuits for different blocks are described in Fig. 4.2.

Astable Multivibrator :

The circuit shown in Fig. 4.2, marked as ①. This is

a simple square wave generator. The output voltage is limited to + V and 0 because of the zener diode. The resistance R_f and capacitor C provide the circuit timing with the amplifier acting as a comparator. The feedback is provided to the non-inverting input by the R_3 and R_4 voltage divider. The input resistor R_1 is to assure high input impedance to the op-amps with input protection. The operation of the circuit is as follows :

When the output switches from negative to positive, the capacitor charges up from negative to positive. When the capacitor reaches the voltage on the non-inverting input, which is + $V_{out} \beta$ ($\beta = R_4/(R_3+R_4)$, $R_1 \gg R_3$ or R_4), the circuit switches negative and the process repeats.

The square wave is made symmetrical by adjusting the value of β and frequency is varied by varying R_f. The set values for 50 Hz is shown in the circuit. The negative half of the square wave is suppressed by the zener diode Z. This is shown in the waveform as Ⓐ.

INVERTER :

A CMOS inverter (74C06) is used to invert this signal Ⓐ to get signal Ⓑ. CMOS chips are being used as they work at the same voltage range as the op-amps and no separate supply is needed. Thus two signals at 180° phase shift is got at the required frequency as shown in the waveform.

High Frequency Modulation Circuit :

In order to avoid the saturation of pulse transformers which are used for isolation of the gate circuit from the power circuit, high frequency modulation of the gate pulses is necessary. A timer circuit NE555 is used for this purpose which is shown in the Fig. 4.2 marked as ②. The frequency of this modulating signal can be adjusted by varying R and C. It is adjusted for approximately 10 KHz. The resulting modulated gate pulses are shown in the waveforms as ⓓ and ⓔ.

Amplifier and Pulse Transformer Isolation :

In order to trigger SCRs reliably, the gates have to be driven hard and the pulse magnitude should be large but within the maximum limits. Each pulse train at points ⓓ and ⓔ is amplified and isolated using a common emitter configuration of a transistor (SL100) amplifier and pulse transformer and fed to the gates of the respective thyristor. The pulse transformer provides isolation for gate pulses. The circuit details are shown in Fig. 4.2 marked as ③.

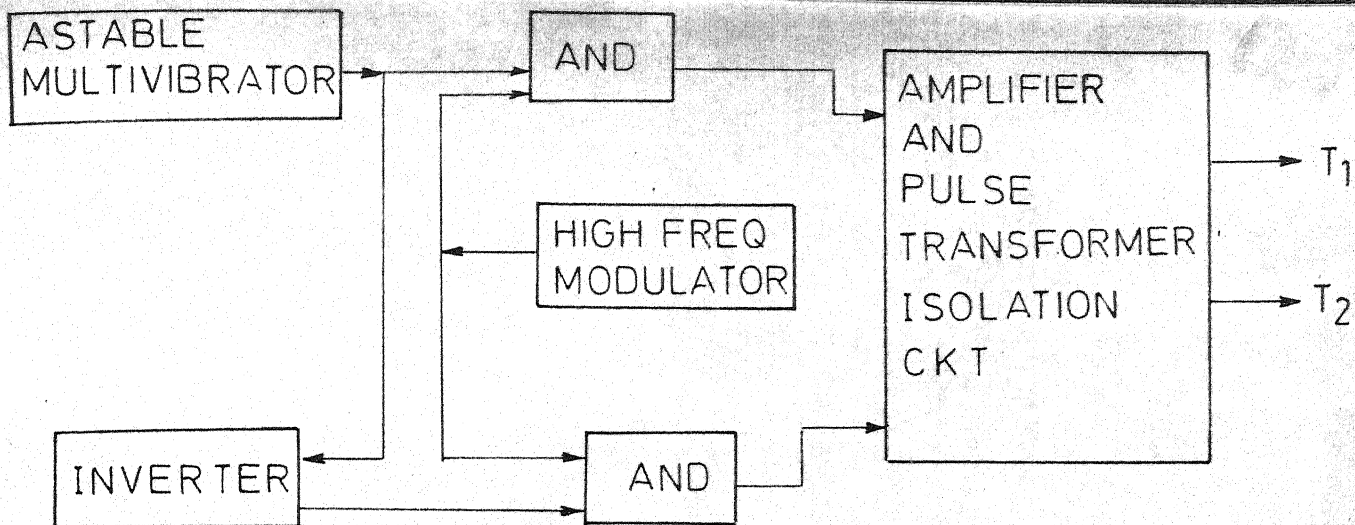Thus a control circuit is developed for an inverter with provision for variable frequency.
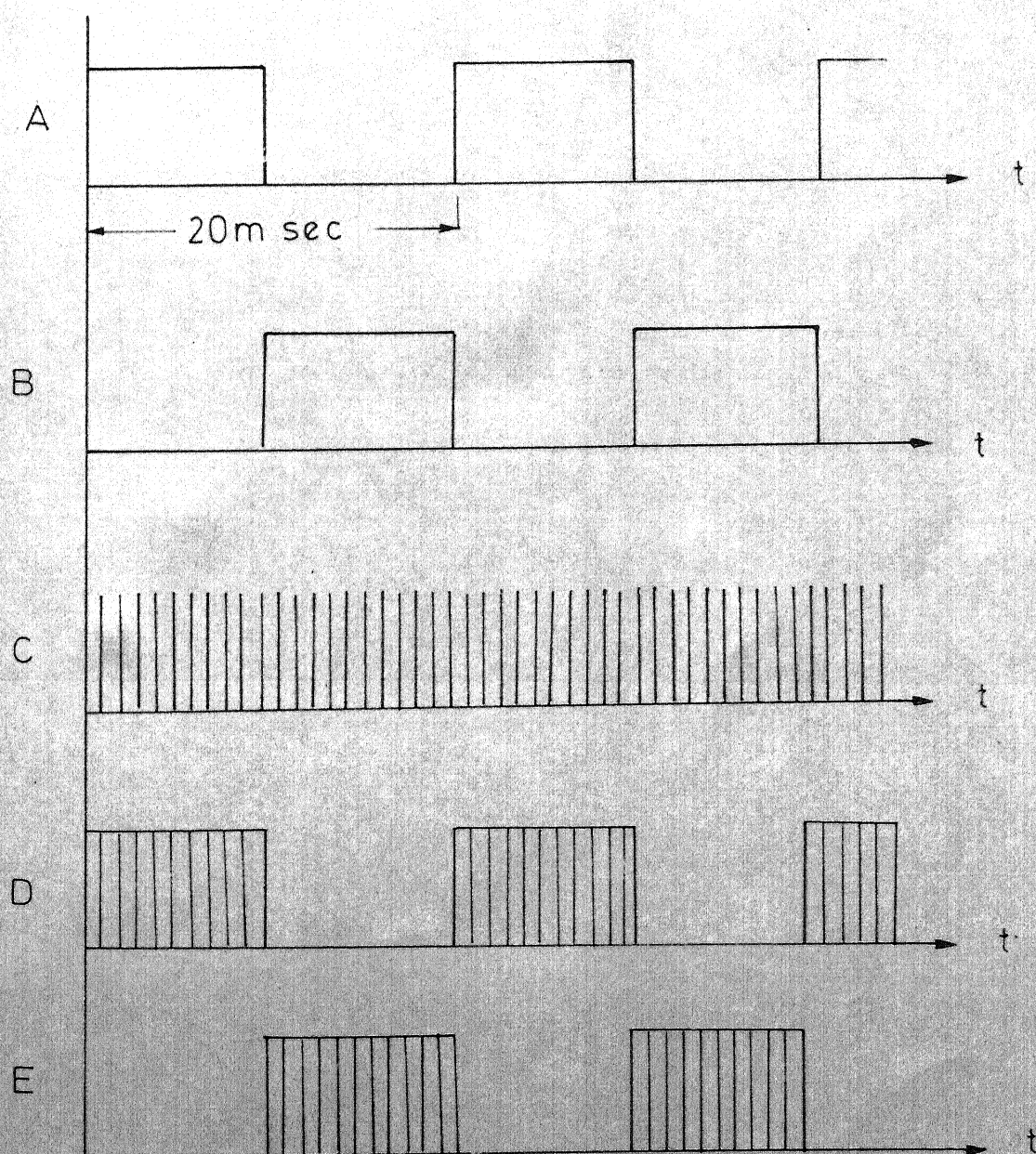
FIG. 4.1(a) BLOCK DIAGRAM OF FIRING SCHEME FOR INVERTER

FIG. 4.1(b) TRIGGERING PULSES TO THYRISTORS IN THE 1-Φ INVERTER
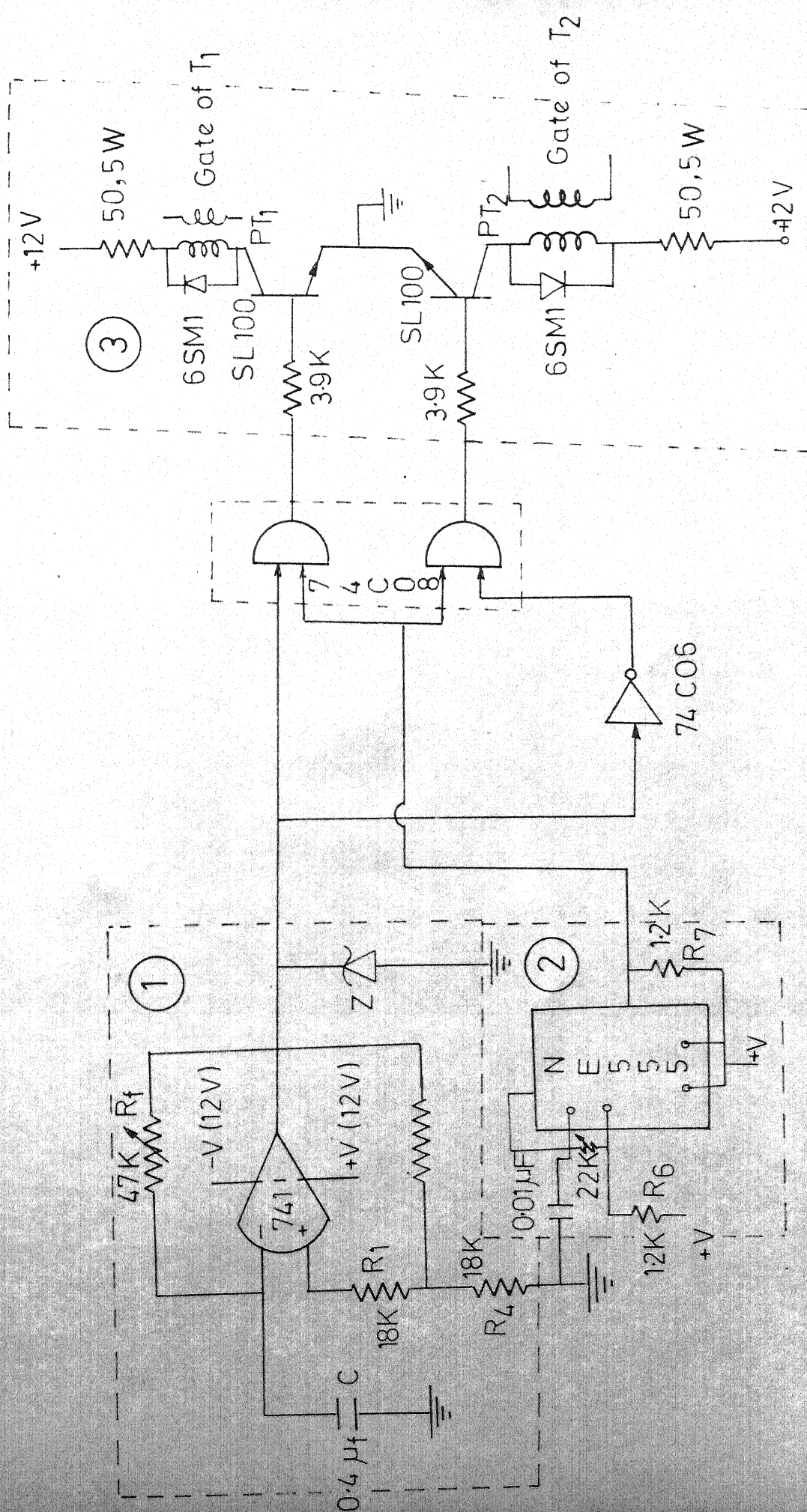
FIG. 4·2 DETAILED CIRCUIT DIAGRAM FOR THE INVERTER

4.3 TRIGGERING CIRCUIT FOR CHOPPER

The main block diagram of the firing circuit for a chopper is shown in Fig. 4.3(a). This gives, the triggering pulses to the thyristors T_{M1}, T_{M2} and T_c as shown in Fig. 4.3(b). The frequency of the chopper is decided by allowing the minimum on and off times of the main thyristor and practical limitations of the commutation circuit components. The frequency for this system was chosen as 250 Hz. The circuit diagram details is shown in Fig. 4.4. An astable multivibrator is used to get a square wave (I) of this frequency. Output of monostable multivibrator which is, triggered at the positive edge of (I), t is applied to the gates of thyristors T_{M1} and T_{M2} after being amplified and isolated by a pulse transformer. The wave (J) is used to generate a ramp (K) of the same frequency and compared with a d.c. signal which can be varied. The output of the comparator (L) is used to trigger a monostable multivibrator. This signal (M) is given to the gate of the auxiliary thyristor T_c after an amplifier and pulse transformer. The on time of the main thyristor can be varied by changing the d.c. signal to the comprator, which will vary the time at which T_c is triggered. The associated circuits for different blocks are described below.

Astable Multivibrator :

The circuit is shown in Fig. 4.4 marked as (1). The working of this circuit has already been described in the previous section. The feedback resistor R_f is adjusted to give a square-wave of 250 Hz. A CMOS monostable multivibrator (74C221) is triggered at the positive going edge of the square wave. The monostable output (J) is used to trigger both the thyristors T_{M1} and T_{M2} by using two different amplifiers and pulse transformers.

Ramp Generator :

The circuit is shown in Fig. 4.4 marked as (2). This is basically an integrator circuit with a slight modification. The input to the inverting terminal of the op-amp is the monostable output (J). The non-inverting terminal is kept at 0.6V by a diode as shown. The feedback path is a parallel combination of a capacitor and a zener diode.

In the circuit, R and C provide the timing, so that adjusting R_1 changes the frequency of operation. Since the voltage on R_1 is + V and O, the summing point voltage of op-amp remains at 0.6 V (due to feedback). The current through R_1 is constant, thus charging the capacitor with constant current. When the inverting terminal is low, the capacitor gets charged linearly to + V and when the input to the inverting terminal is high, the discharge resistance (R_1) being low, the capacitor discharges very fast. Thus the waveform

(K) is obtained.

This ramp is compared with a d.c. level with the help of an op-amp comparator as shown in Fig. 4.4, marked (3). The output of the comparator (L) is inverted with the help of a CMOS NAND gate (74C00) and fed to a monostable multivibrator (74C221). It triggers the monostable at the positive edge (M) and this signal is applied to the auxiliary thyristor T_c.

Amplifier and Pulse Transformer :

The monostable outputs (J) and (M) are amplified using a transistor SL100 with common emitter configuration and applied to the gates through pulse transformers. Pulse transformers are used at the output stage to provide isolation. This is shown in Fig. 4.6 marked as (4).

Thus a reliable triggering circuit has been designed for the chopper. But this does not provide the precaution necessary while starting the choppers. When the triggering pulses are given to the thyristors, it should be ensured that the cummutating capacitor is charged initially. If this is not done, commutation failure will take place and large short circuit current will flow, which may damage the thyristors. To avoid this, the auxiliary thyristor must be triggered first, so that the commutating capacitor gets charged. This is done by incorporating a time delay circuit in the firing scheme.
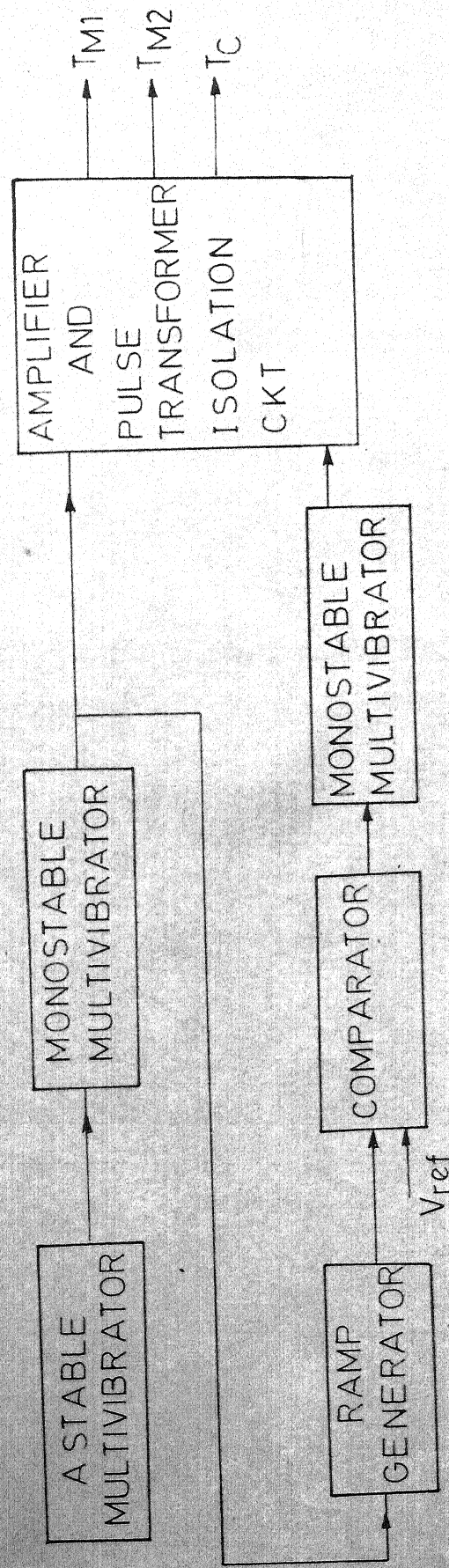
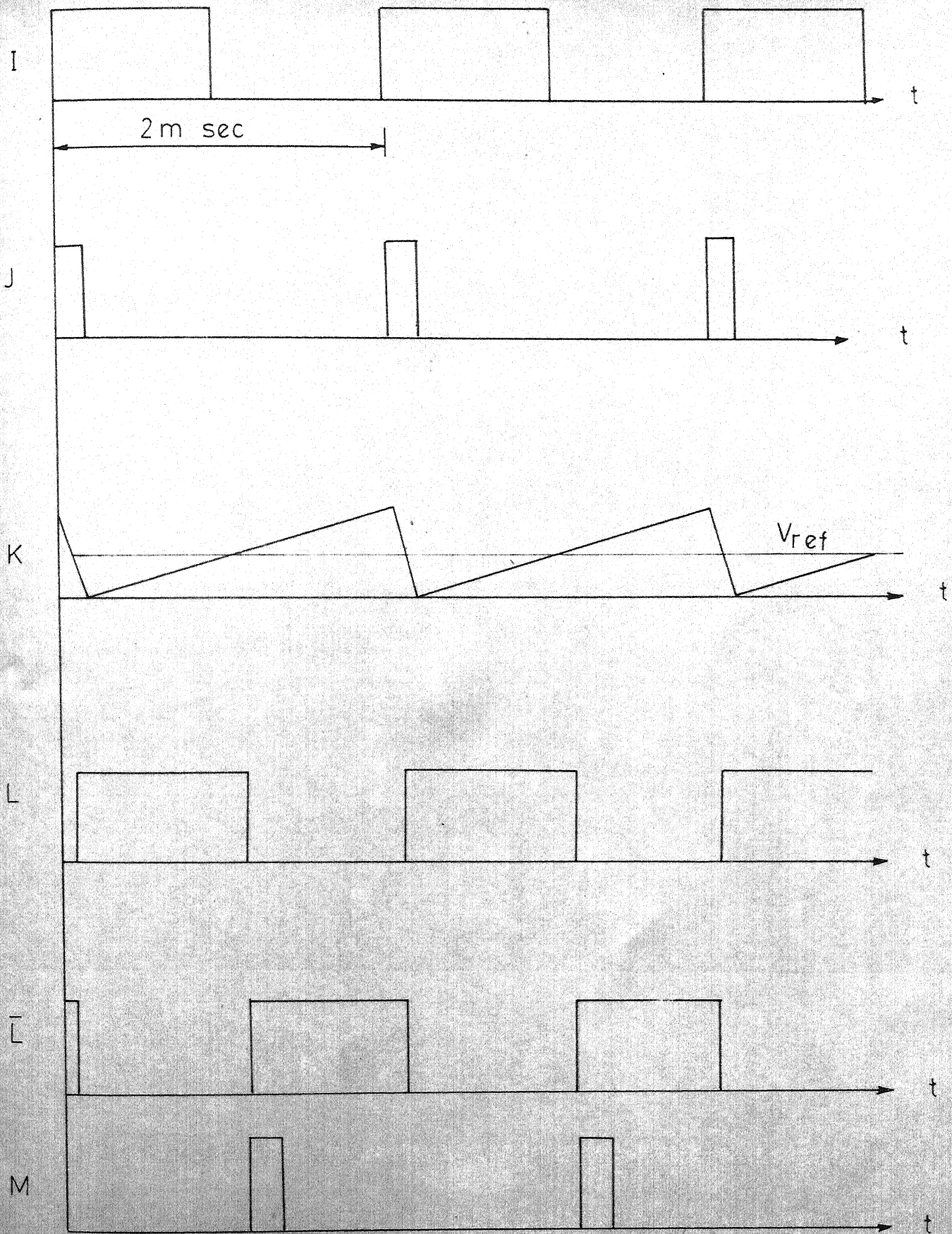FIG. 4.3(a) BLOCK DIAGRAM OF FIRING SCHEME FOR CHOPPER

FIG. 4.3 (b) TRIGGERING PULSES TO THYRISTORS IN THE STEP UP CHOPPER

58
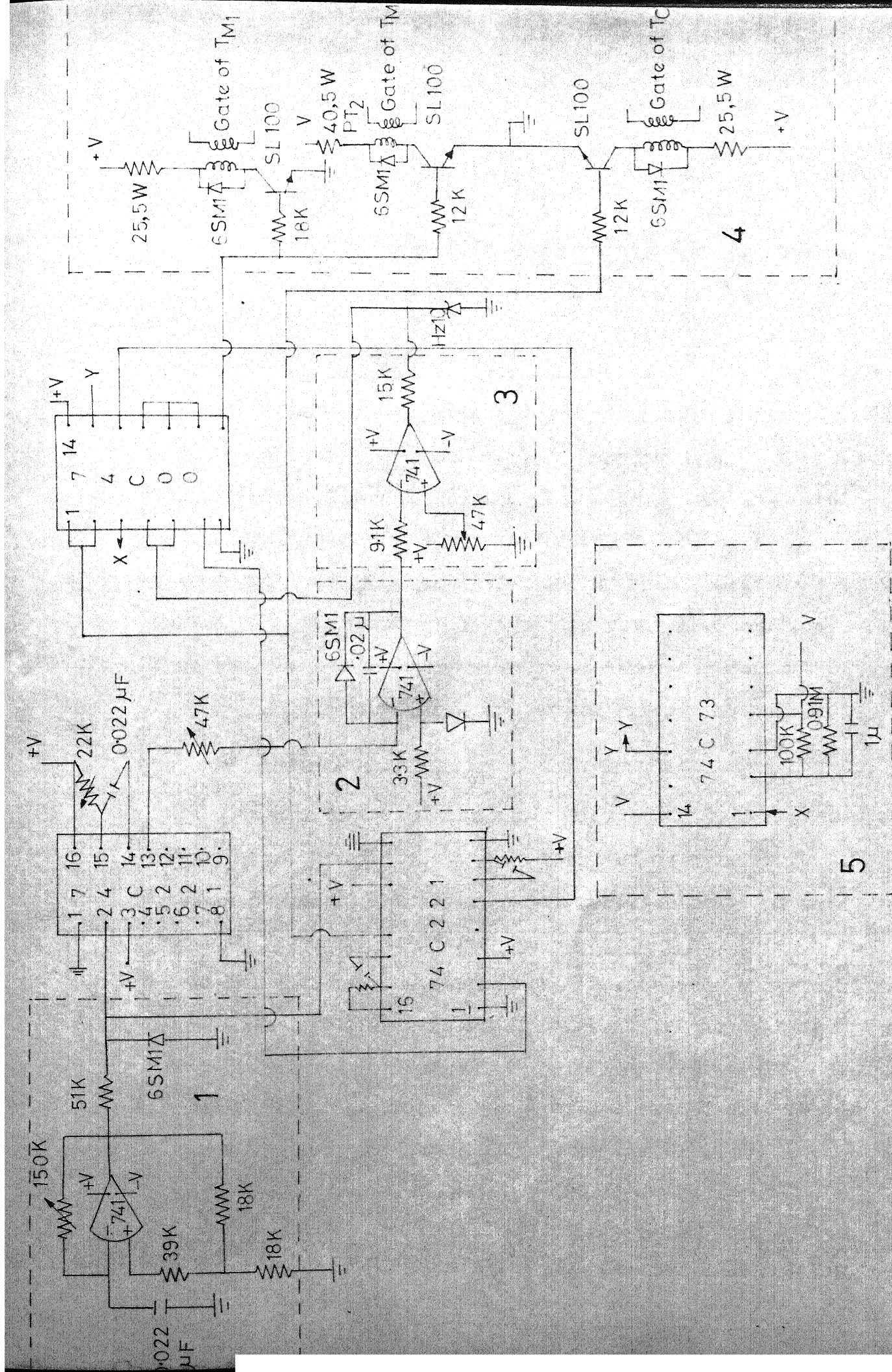
FIG. 4.4 DETAILED CIRCUIT DIAGRAM FOR THE CHOPPER

Time Delay Circuit :

A J-K flip-flop (74C73) shown in the Fig. 4.4 marked as ⑤ is used to give the time delay between the pulses to auxiliary and main thyristor. The delay time is set by the charging of an R-C circuit. The triggering signal to the main thyristors T_{M1} and T_{M2} are given through the flip-flop and directly to the auxiliary thyristor T_c. When the triggering signals are applied, T_{M1} and T_{M2} get the gate pulses only after the capacitor of the R-C circuit is charges to + V and sets the flip-flop. During this time, the commutating capacitor gets charged and is ready for commutation. Thus the problem of short circuit is taken care of. The time delay incorporated in the actual circuit is 1 msec.

4.4 CONCLUSIONS

A design scheme of the triggering circuit, for a single-phase inverter and d.c. step up chopper has been explained in this chapter. The inverter triggering circuit is a variable frequency triggering pulse circuit and is simple to design with minimum components. The chopper triggering circuit has a variable on-time, constant frequency triggering pulse and with slight changes, variation in frequency can be achieved. The inherent problem of short circuit in the chopper has been over come by a delay circuit.

analysed to predict the speed-torque characteristics of a 1-ϕ induction motor using equivalent circuit model. Since the input to the induction motor is non-sinusoidal, harmonic components are also generated. These components are determined using harmonic equivalent circuits based on the Fourier series approach. The motor is modelled by the conventional equivalent circuit fore each of the harmonic frequencies, using appropriate value of slip for such frequency. The study reveals that the magnetization characteristic of the motor gets saturated as the current increases. The saturating effect is quite predominant at higher values of current. The torque-speed characteristics are obtained considering saturation effects. Some qualitative explanation is given with regard to harmonic magnetizing inductance when the fundamental magnetizing inductance saturates. The effect of harmonics on the torque-speed characteristics is also studied. Lastly, the torque-speed characteristics obtained from the experimental set-up are compared with the theoretical characteristics.

5.2 DETERMINATION OF DIFFERENT MODES IN 1-ϕ PARALLEL INVERTER WITH SERIES DIODES

Figure 5.1 shows the circuit diagram of the modified parallel inverter. It is seen that continuity of the direct current fed through L_d forces atleast one of the thyristors T_1 or T_2 to conduct at all times. Further,

capacitor C allows only one thyristor at a time to conduct. During the half cycle in which T_1 is conducting, the equivalent circuit of the inverter is as shown in Fig. 5.2, which can be further reduced to one of the three topological modes :

Mode I: Diode D_1 blocking and diode D_2 conducting

Mode II:Both diodes conducting

Mode III : Diode D_1 conducting and diode D_2 blocking

The load consisting of a sinusoidal counter emf in series with an inductance is assumed as a simplified representation of a motor. The capacitor voltage v_c must be initially positive and must become negative before the end of the half cycle. A similar set of three modes can occur in the other half cycle when thyristor T_2 is conducting :

Mode I'   Diode D_2 blocking and diode D_1 conducting

Mode II'   Both diodes conducting

Mode III'   Diode D_2 conducting and diode D_1 blocking

With the following modifications, the same equations can be used for the half cycle in which T_2 is conducting : (a) the counter emf is reversed,(b) the capacitor voltage is reversed, and (c) currents i_1 and i_2 in the diodes D_1 and D_2 are interchanged. Therefore, only the equations for modes I, II and III are to be solved and the other half cycle can be taken care of with the above modification.
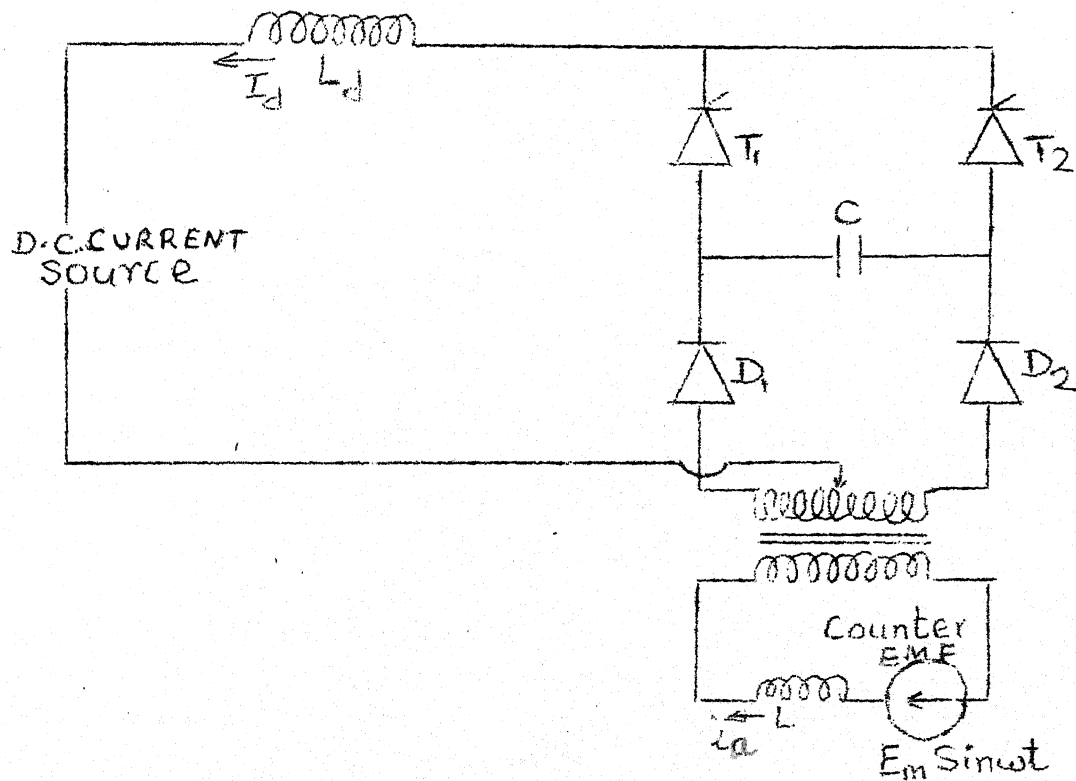
Fig. 5·1 SINGLE PHASE CURRENT FED INVERTER WITH LOAD
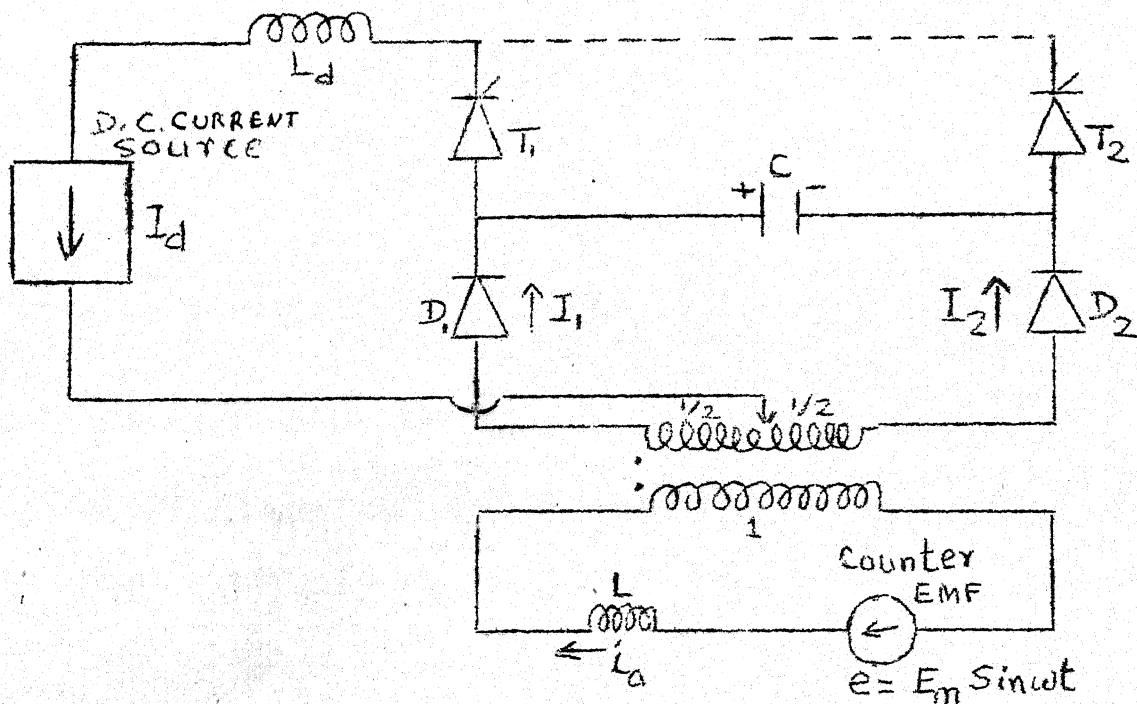
Fig. 5·2 EQUIVALENT CIRCUIT WITH T_1 CONDUCTING.

In the equations to be developed for each of the modes, the time zero is assumed to be at the beginning of the mode. Thus when using the results, the time zero must be redefined. The following initial conditions must be redefined at the start of each mode, being the final values of the previous modes.

Θ = initial phase lag angle with respect to counter emf e

V_i = initial value of capacitor voltage v_c

I_i = initial value of current i_2 in diode D_2

Here, the current i_2 is chosen arbitrarily as the state variable and other currents i_1 and i_a are related to i_2 by the following identities in all modes.

$$\text{Direct current } I_d = i_1 + i_2 \tag{5.1}$$

$$\text{Instantaneous load current } i_a = \tfrac{1}{2}(i_1 - i_2) \tag{5.2}$$

The equation for the counter emf remains the same for all the modes, although time t and Θ are to be redefined at the start of each mode.

$$e = E_m \sin(\omega t + \Theta)$$

The analysis is carried out in the normalized form, with the selection of peak counter emf E_m as the base value.

Base voltage $- E_m$

Base angular frequency $- \omega_0 = \dfrac{1}{\sqrt{LC}}$

Base impedance $- X_o = \sqrt{\dfrac{L}{C}}$

Base current $- I_o = \dfrac{E_m}{X_m} = E_m \sqrt{\dfrac{C}{L}}$

A parameter K is defined which is the ratio of the operating frequency ω to the base frequency ω_o.

$$K = \omega/\omega_o$$

5.2.1 Mode I :

Thyristor T_1 and D_2 are conducting, D_1 and T_2 are blocking. During this mode, the equivalent circuit comprises of transformer, diode D_2, capacitor C, thyristor T_1 and inductance L_d. The capacitor C discharges linearly as constant dc current passes, from its initial voltage V_i. The load current in the secondary is also of constant magnitude and therefore no voltage is induced in the load inductance L.

$$i_1 = 0 \qquad\qquad\qquad (5.4)$$

$$i_2 = I_i = I_d \qquad\qquad\qquad (5.5)$$

$$i_a = \tfrac{1}{2}(i_1 - i_2) = - \frac{I_d}{2} \qquad\qquad (5.6)$$

$$C \frac{dV_c}{dt} = - I_d$$

or

$$V_c = V_i - \frac{I_d}{c} \cdot t \qquad\qquad\qquad (5.7)$$

For Mode I to continue, capacitor voltage V_c must exceed e i.e.,

$$v_c \ > \ e$$

When v_c becomes less than e, diode D_1 starts conducting and Mode II starts. Before v_c becomes less than e, if T_2 is triggered, Mode III' starts. But this is possible only if v_c is less than zero at that time.

5.2.2 Mode II :

Thyristor T_1, diode D_1 and diode D_2 are conducting, thyristor T_2 is blocking. Here, the initial condition for $I_i = I_d$, if the previous mode was Mode I and $I_i = 0$ if previous mode was Mode III. For both the previous modes, $V_i = E_m \sin \Theta$.

The following are the equations for this mode :

$$L \frac{di_2}{dt} = v_c - e \tag{5.8}$$

$$C \frac{dV_c}{dt} = -i_2 \tag{5.9}$$

Taking Laplace transforms, we get

$$s\, i_2(s) - I_i = \frac{V_c(s) - e(s)}{L} \tag{5.10}$$

$$s\, V_c(s) - V_i = \frac{-i_2(s)}{C} \tag{5.11}$$

Solving the above simultaneous equations for $i_2(s)$ and $V_c(s)$, and taking the Laplace inversion of it, we get

$$v_c(t) = -\left[\frac{I_i}{\omega_0 C} + \frac{\omega_0 \omega}{\omega_0^2 - \omega^2} E_m \cos \theta\right] \sin \omega_0 t$$

$$-\left[\frac{\omega_0^2}{\omega_0^2 - \omega^2} \cdot E_m \sin \theta - V_i\right] \cos \omega_0 t$$

$$+ \frac{\omega_0^2}{\omega_0^2 - \omega^2} E_m \sin(\omega t + \theta) \tag{5.12}$$

and $i_2(t) = -C\frac{dV_c}{dt} = \left[I_i + \frac{\omega_0^2}{\omega_0^2 - \omega^2} C E_m \cos \theta\right] \cos \omega_0 t$

$$- \omega_0 C\left[\frac{\omega_0^2}{\omega_0^2 - \omega^2} E_m \sin \theta - V_i\right] \sin \omega_0 t -$$

$$\frac{\omega_0^2}{\omega_0^2 - \omega^2} C E_m \cos(\omega t + \theta) \tag{5.13}$$

Current $i_1 = I_d - i_2$ $\hspace{3cm}$ (5.14)

For this mode to end,

(a) $i_2 = 0$ before $i_1 = 0$, Mode III follows

(b) $i_1 = 0$ before $i_2 = 0$, Mode I follows

(c)   thyristor T_2 is fired before current zero occur, but v_c has become negatives, Mode 2' follows.

5.2.3 Mode III :

Thyristor T_1 and diode D_1 are conducting, thyristor T_2 and diode D_2 are blocking. The circuit for this mode comprises of transformer, diode D_1, thyristor T_1 and L_d. Capacitor voltage remains constant and as load current is constant, no

voltage is induced in the load inductance L.

The following are the equations for this mode :

$$i_1 = I_d \qquad\qquad (5.15)$$

$$i_2 = I_i = 0 \qquad\qquad (5.16)$$

$$i_a = \tfrac{1}{2}(i_1 - i_2) = \frac{I_d}{2} \qquad\qquad (5.17)$$

$$v_c = V_i \qquad\qquad (5.18)$$

This mode continues till the capacitor voltage v_c is less than the counter emf e. If $v_c >$ e, diode D_2 starts conducting and mode II starts. If T_2 is fired before $v_c >$ e, then mode I' starts.

The above procedure to compute the various voltages and currents can be easily implemented in the digital computer. The waveforms obtained by this method is shown in Fig. 5.3(a) and the oscillographs are shown in Fig. 5.3(b). In the present application, the operation at the constant frequency is fixed. For this frequency, it was observed that with the change of I_d, only the amplitude of i_a, v_c and e changed but the modes of operation were I, II, III.

5.3 DETERMINATION OF TORQUE-SPEED CHARACTERISTICS OF A 1-ϕ INDUCTION MOTOR

The performance equations of a single-phase machine can be derived from its equivalent circuit, using the double
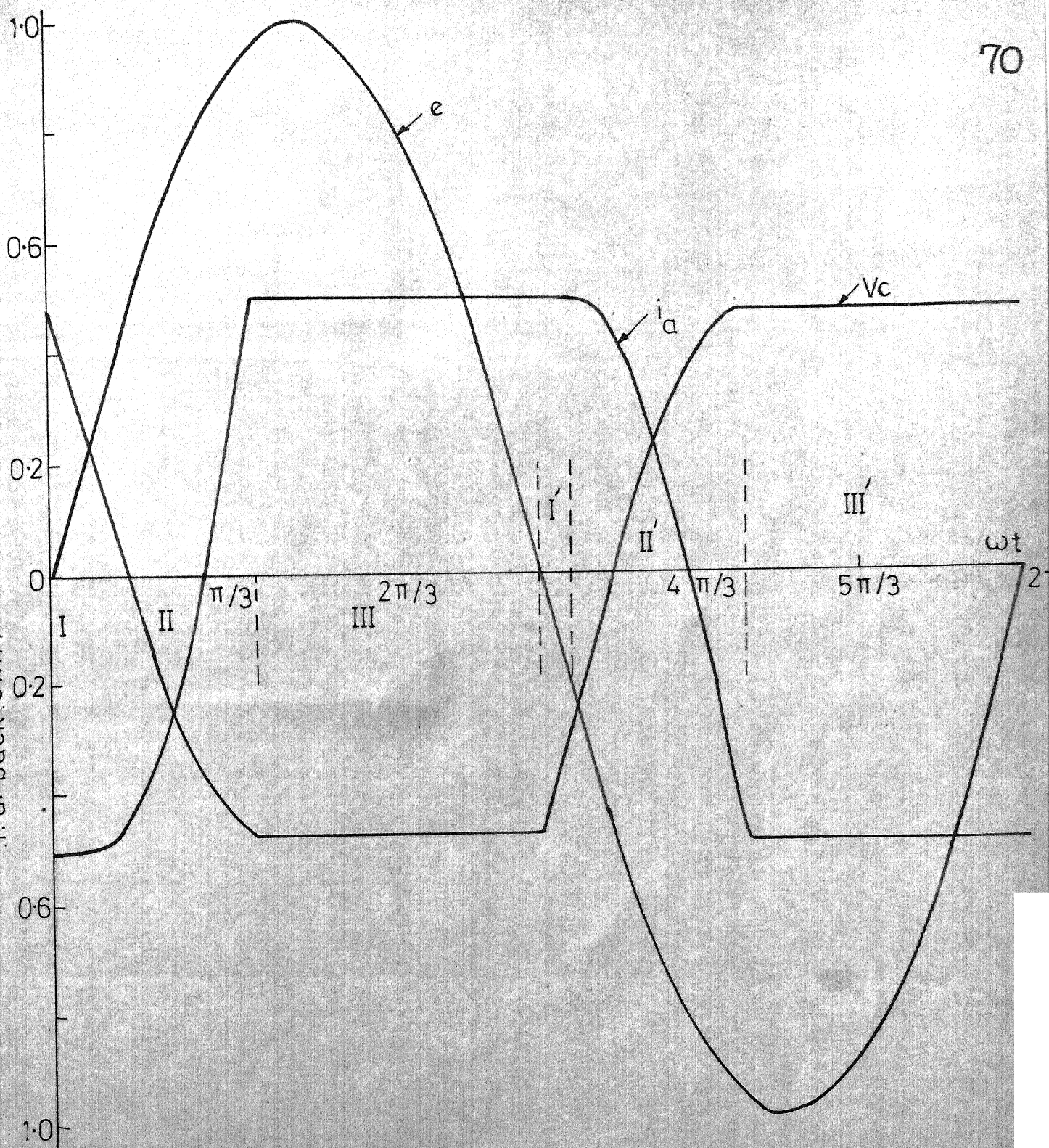
FIG.5·3 (a) WAVEFORMS FOR $\omega/\omega_o = 1\cdot0$, $I_d = 1\cdot0$ p.u WITH DIFFERENT MODES
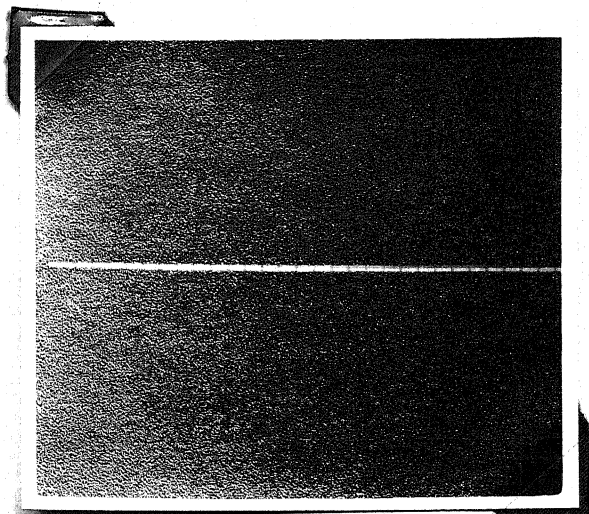
Fig. 5.3 (b) (i)

Fig. 5.3 (b) (ii)

Inverter capacitor voltage
Scale: X-Axis - 5 msec/cm
       Y-Axis - 100 V/cm.
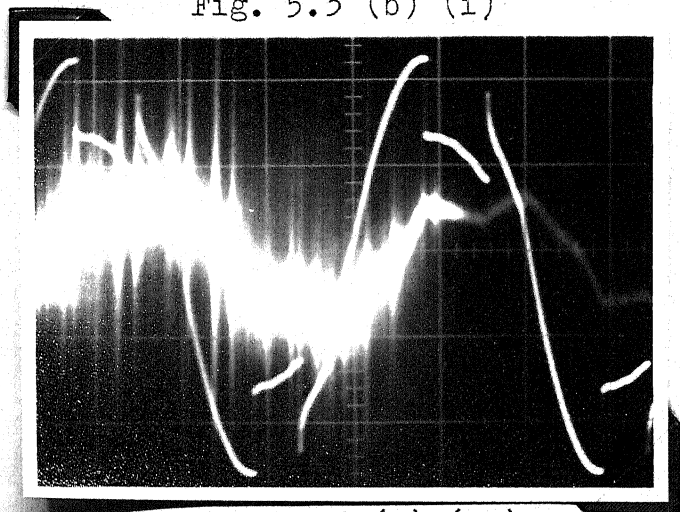
Load voltage and load current
Scale : X-Axis - 5 msec/cm
         Y-Axis - 10 mV/cm for
                  current
               - 100 V/cm for
                  voltage

revolving field theory. When the stator is excited by a single-phase supply, a pulsating field is produced. This pulsating field, for the analysis purpose, can be resolved into two fields rotating in opposite directions at synchronous speed. The amplitude of each field is one-half of that of the main field. When the machine is at standstill, torques equal in magnitude and opposite in direction are produced by these two fields. Therefore, there is no resultant torque for starting. Once it is started, the field which is rotating in the same direction as that of the rotor constitutes the main field while the backward field decreases to a negligible value. The slip of the rotor with respect to the forward field is given by $S_f = \dfrac{n_s - n}{n_s}$ and the slip of the rotor with respect to the backward field is given by $S_b = \dfrac{n_s + n}{n_s}$. $= 2 - S_f$ where n_s and n are the synchronous and rotor speed respectively.

The load current obtained from the single phase current source inverter is somewhat a squarewave. By Fourier analysis, this can be represented by a fundamental together with a series of time harmonics. The waveform, possessing half-wave symmetry does not contain any even harmonics. The odd harmonic currents produce torque which alternately aids and opposes the fundamental torque (17). Moreover, these torques are quite small compared to the rated torque and the total is negligibly small negative torque. The slip of the rotor for

the Nth harmonic stator excitation is $S_{N} \pm = \dfrac{N \pm (S_f - 1)}{N}$

(positive sign for the forward field) and negative sign for the backward field). If the motor speed varies from synchronous speed to standstill, the fundamental slip, S_f, varies from 0 to 1, but for the third and fifth harmonics, S_3 and S_5 varies from 0.67 to 1 and 0.8 to 1. Thus the total harmonic torques, which is very low, affects the overall torque at very high slip(18). The normal working range of the motor is from $S = 0$ to $S = 0.2$ and so the harmonic torques can be neglected.

5.3.1 Method of Analysis

The load current is not sinusoidal. After the steady sequence of modes has been determined, the load current can be written in a general form

$$i_a(x) = \frac{a_0}{2} + \sum_{n=1}^{\infty} (a_n \cos n\,x + b_n \sin nx) \qquad (5.19)$$

where $a_0 = 0$, as there is no d.c. component, a_n and b_n are defined as follows :

$$a_n = \frac{1}{\pi} \int_0^{2\pi} i(x) \cos nx\; dx \qquad (5.20a)$$

$$b_n = \frac{1}{\pi} \int_0^{2\pi} i(x) \sin nx\; dx \qquad (5.20b)$$

The resultant peak magnitude I_m is given by

$$I_m = \sqrt{a_n^2 + b_n^2} \qquad\qquad (5.21a)$$

and phase angle $\phi = \tan^{-1}(-\frac{a_n}{b_n}) \qquad\qquad (5.21b)$

The torque speed characteristics are obtained by considering : (i) Total rms current, (ii) Fundamental rms current.

The equivalent circuit shown in Fig. 5.4 is valid for sinusoidal supply. Here the inverter is fed by a current source. For a given source current, for low values of slip all the source current must flow through the magnetising reactance X_{m1}. This will saturate X_{m1}. It is therefore necessary to incorporate saturation of X_{m1} in the analysis. This is very much required for the magnetizing branch especially when slip increases.

The open circuit magnetization characteristic is shown in Fig. 5.5. The dotted portion is obtained after correcting for the drops across stator impedance and backward parallel branch. This curve also represents the relation between the fundamental frequency flux linkage of the stator windings to the fundamental frequency magnetizing current. Therefore, in per unit system operating point slope gives the fundamental magnetizing inductance. Because the forward and backward
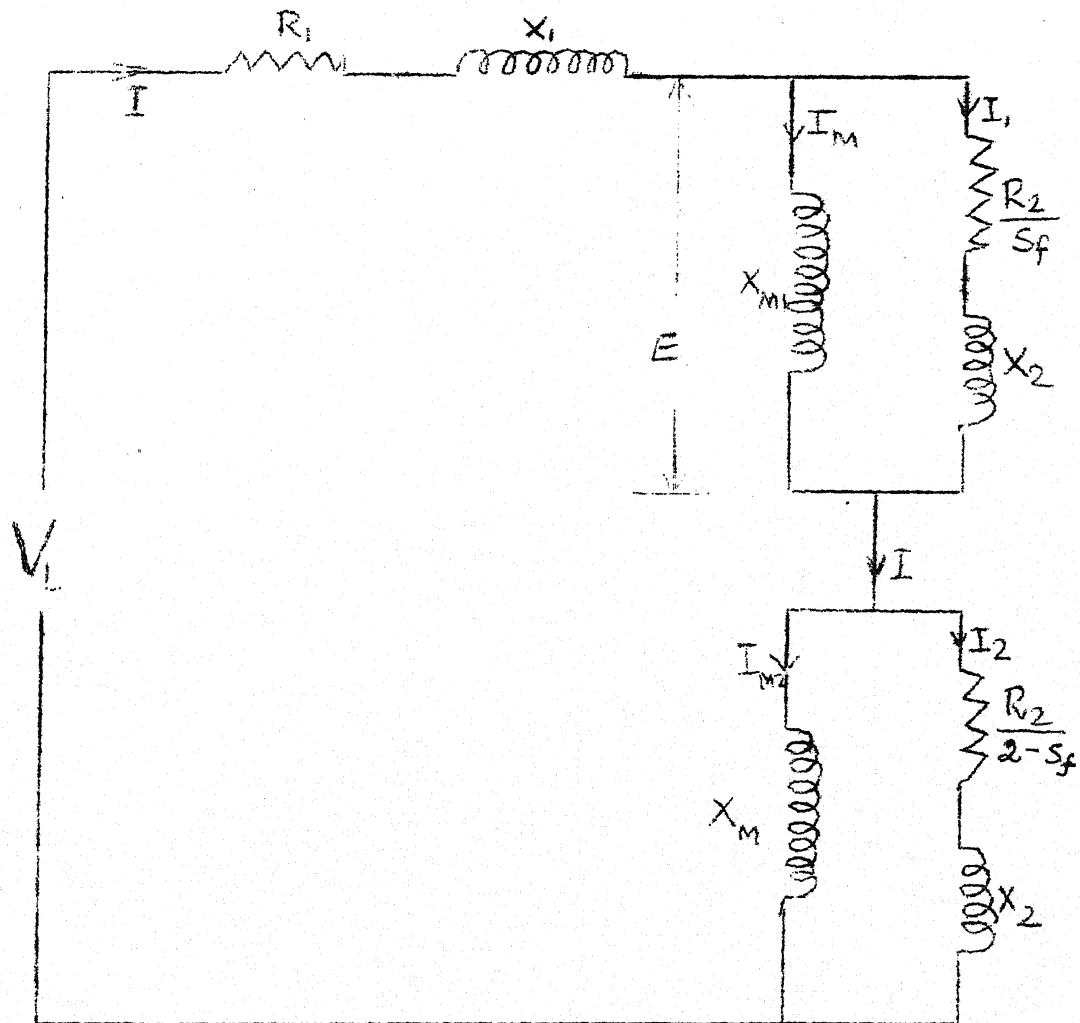
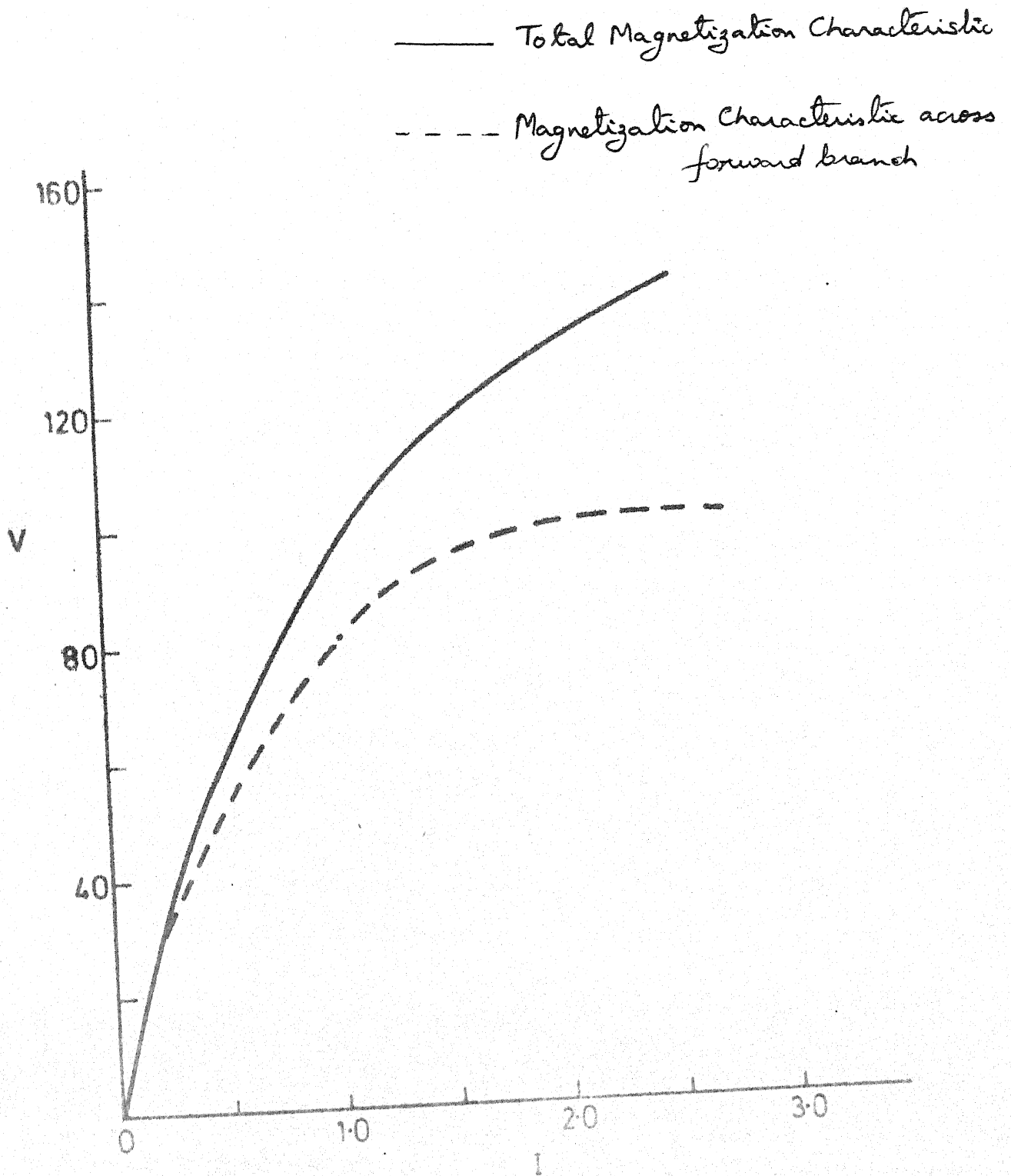Fig. 5.4 EQUIVALENT CIRCUIT OF SINGLE
PHASE INDUCTION MOTOR

FIG·5·5 NO-LOAD MAGNETIZATION CHARACTERISTICS

revolving harmonic mmf space vectors have almost the same
magnitude as the fundamental slip varies from 1 to 0, they do
not produce either amplitude or phase modulation of the funda-
mental space vector. Hence the harmonic magnetizing inductance
is the same as the fundamental magnetizing inductance.

To obtain X_{M1} which is a function of i_a, the single-
phase induction motor is run at synchronous speed with the
help of a d.c. shunt motor which is coupled to it. Keeping it
at synchronous speed, some known a.c. voltage V is applied
to the stator of the induction motor and the a.c. current I
is noted. The equivalent circuit at the synchronous speed is
shown in Fig. 5.6. Except X_{M1}, all the other values in Fig.
5.6 are obtained from the usual tests described in Appendix A.
Thus X_{M1} is found for a particular current. Stator voltage
of the induction motor is varied and X_{M1} is computed, keeping
the speed at synchronous speed. Thus the value of X_{M1} as a
function of current is obtained.

For a particular value of p.u. link current I_d, the steady
state waveform of the inverter load current is determined as
explained in Section 5.2. Now, it is necessary to determine
the torque producing component of current for both forward
and backward fields. This can be obtained from the equivalent
circuit of Fig. 5.4. Once the current is computed the slip
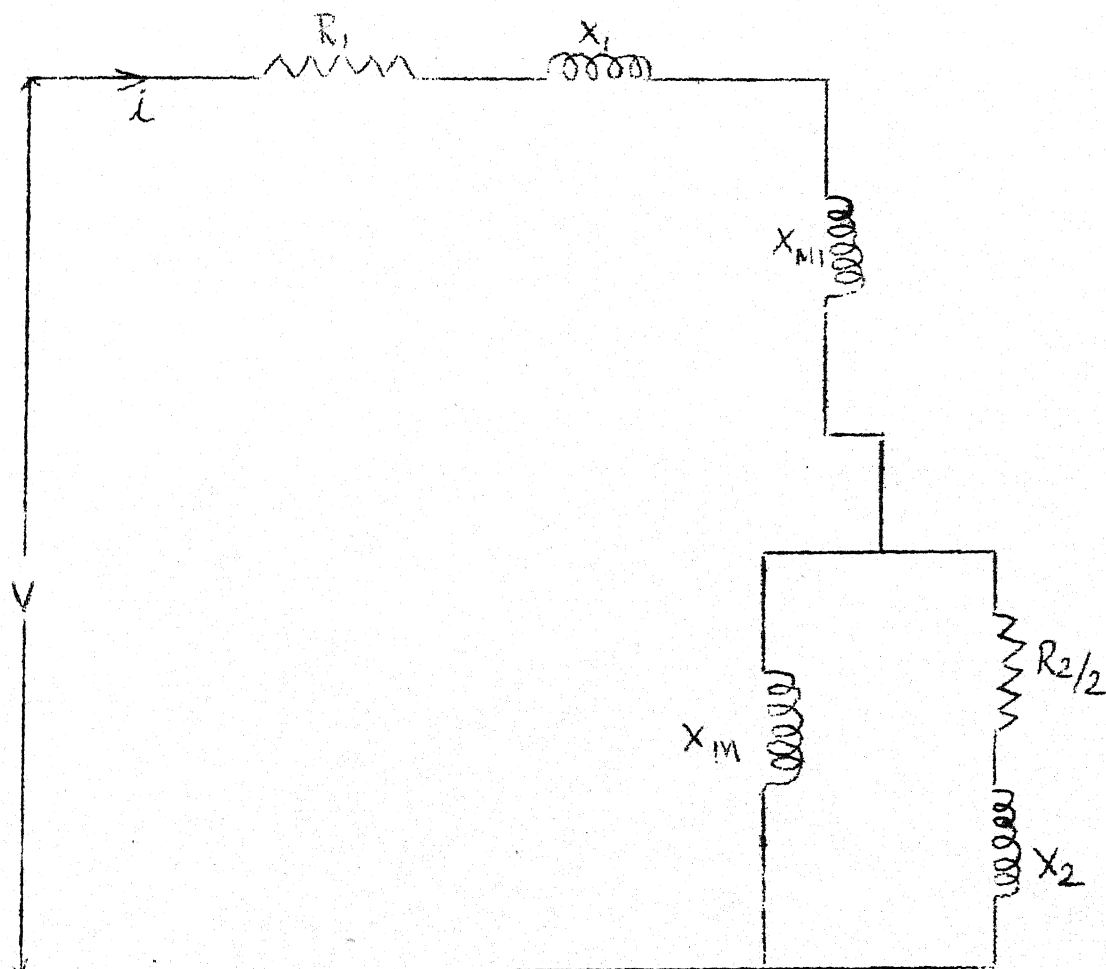and effective torque can be determined as explained below :

Fig. 5.6 EQUIVALENT CIRCUIT OF SINGLE
PHASE INDUCTION MOTOR AT SYNCHRONOUS
SPEED

Let E be the voltage across the forward branch

X_{M1} is the magnetizing reactance at current I_M

I — rms motor current (or fundamental rms current as the case may be)

I_1 — current through R_2/S_f

I_2 — current through $R_2/2-S_f$

$$E = I_M X_{M1} = I_1 \sqrt{(\frac{R_2}{S_f})^2 + (X_2)^2} \tag{5.22}$$

$$I_1 = \frac{I X_{M1}}{\sqrt{(\frac{R_2}{S_f})^2 + (X_{M1} + X_2)^2}} \tag{5.23}$$

$$(I X_{M1})^2 = I_1^2 \left[(\frac{R_2}{S_f})^2 + (X_{M1}^2 + X_2^2 + 2X_{M1} X_2)\right] \tag{5.24}$$

Substituting (5.22) in the equation (5.24), we get

$$(I X_{M1})^2 = I_1^2 \left[X_{M1}^2 + 2X_{M1} X_2\right] + (I_M X_{M1})^2 \tag{5.25}$$

Therefore,

$$I_1 = \sqrt{\frac{I^2 - I_M^2}{1 + \frac{2X_2}{X_{M1}}}} \tag{5.26}$$

From Eqn. (5.22),

$$(\frac{R_2}{S_f}) = \sqrt{(\frac{E}{I_1})^2 - X_2^2} \tag{5.27}$$

i.e. $\qquad S_f = \dfrac{R_2}{\sqrt{(\frac{E}{I_1})^2 - X_2^2}}$ (5.28)

Forward torque $\quad T_F = I_1^2 \dfrac{R_2}{S_F}$ (5.29)

$I_2 = \dfrac{I\, X_M}{\sqrt{(\frac{R_2}{2-S_f})^2 + (X_M + X_2)^2}}$ (5.30)

Backward torque $T_B = I_2^2 \dfrac{R_2}{2-S_f}$ (5.31)

Total Torque $T = T_F - T_B$ (5.32)

The procedure which is followed for obtaining the effective torque can be summarized as :

1) Machine parameters and the value of X_{M1} as function of I_M is obtained

2) RMS load current (or rms fundamental current as the case may be) is calculated by Fourier analysis as given by eqns. (5.19) to (5.21).

3) A small value of I_M is chosen and $X_M (I_M)$ is obtained from the graph.

4) I_1 is calculated from eqn. (5.26).

5) S_f and T_f are calculated from eqn. (5.28) and (5.29).

6) T_B and T are calculated from eqns. (5.31) and (5.32).

The various points of the speed torque characteristics are calculated following the above mentioned steps, until synchronous speed is reached. At synchronous speed $I_m \approx I$.

This condition is utilised to find out when synchronous speed is reached.

The above method for computing total torque is simple and easy to implement in a digital computer. The results obtained by this procedure are discussed below.

5.4 COMPARISON OF PREDICTED AND EXPERIMENTAL RESULTS

The torque-speed characteristic of the $1-\phi$ induction motor is obtained. These results are compared with the experimental values obtained by the loading test conducted on a single-phase capacitor start induction motor.

The details of the machine are given below :

230 V, $1-\phi$, 0.25 hp

$R_1 = 7.63$ Ohms $\qquad X_1 = 15.52$ Ohms

$R_2 = 4.5$ Ohms $\qquad X_2 = 7.76$ Ohms, $X_M = 84.22$ Ohms

The above parameters of the machine are obtained from the usuals tests as described in Appendix A. The variation of X_{M1} with I_M is shown in Fig. 5.7. The speed-torque characteristics of the machine are obtained using the above procedure as shown in Fig. 5.8. The experimental values are also marked in the figure. The experimental results compare better with the speed-torque characteristics calculated using fundamental rms current rather than the total rms current. This shows that the harmonic currents do not appreciably effect the torque-speed curves.
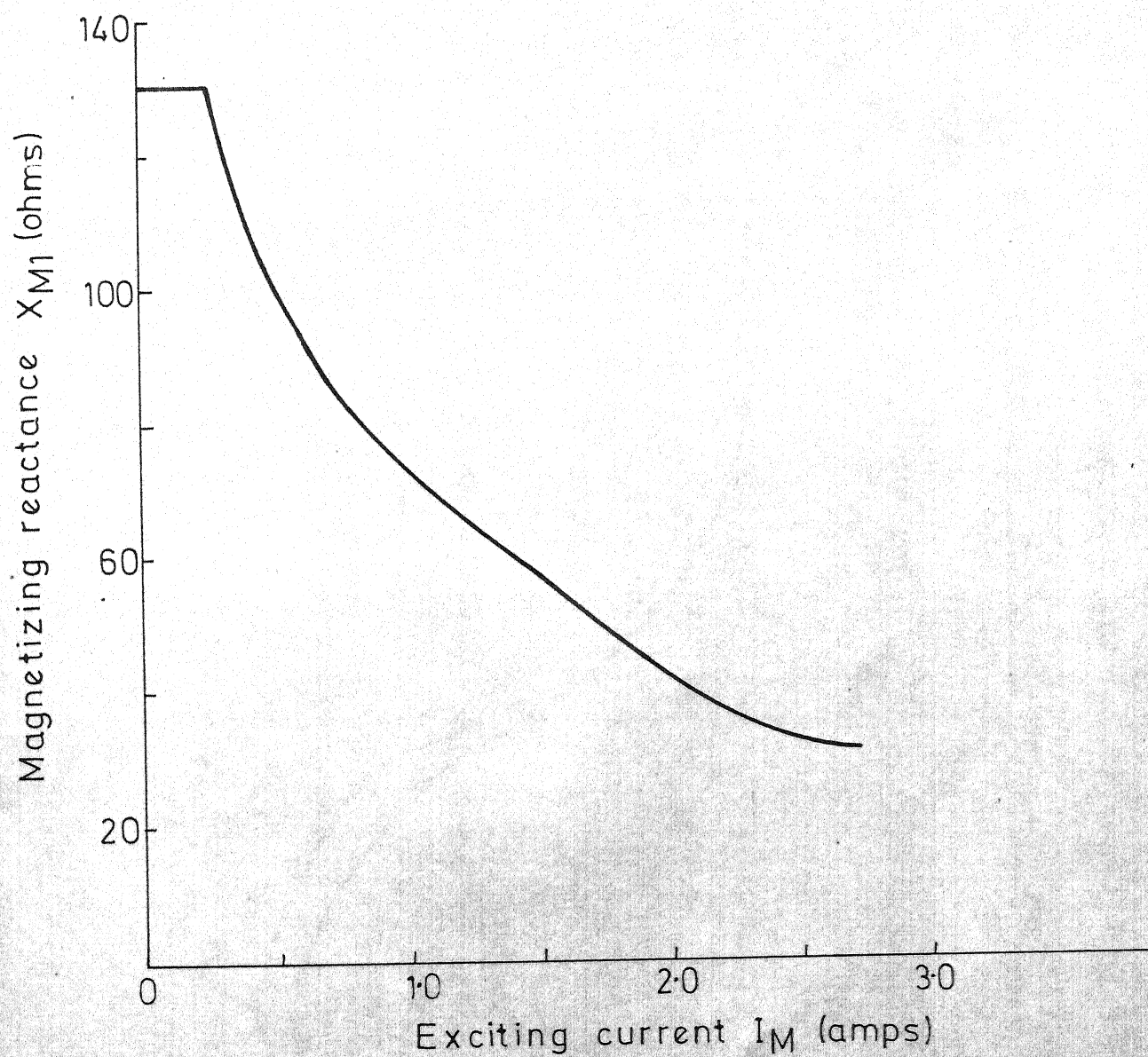
FIG. 5·7 VARIATION OF MAGNETIZATION REACTANCE
WITH EXCITING CURRENT

FIG 5-6 (a) TORQUE SPEED CHARACTERISTICS OF SINGLE PHASE MACHINE WITH $I_d = 1$ p.u.

COMPUTED WITH TOTAL ———— ($I_{RMS} = 2.24 A$)
RMS CURRENT

COMPUTED WITH FUNDAMENTAL – – – – ($I_{RMS} = 2.17 A$)
RMS CURRENT

EXPERIMENTAL x x x

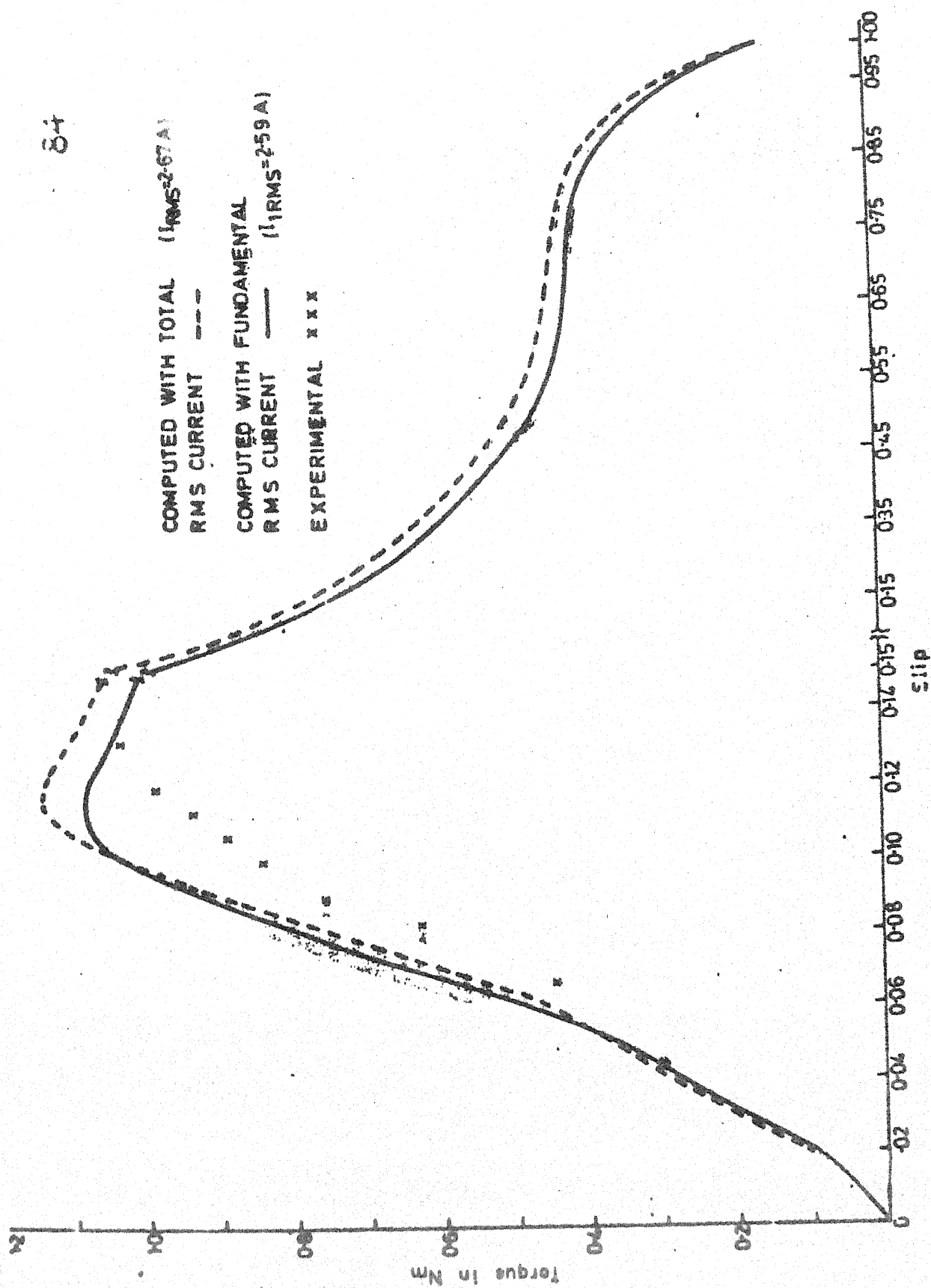FIG 5·6 (b) TORQUE SPEED CHARACTERISTICS OF SINGLE PHASE MACHINE WITH $I_d = 1.2$ p.u.

FIG-5-8 (a) TORQUE SPEED CHARACTERISTICS OF SINGLE PHASE MACHINE WITH $L_d = 1.3$ p.u.

COMPUTED WITH TOTAL ($I_{RMS} = 2.89$ A)
RMS CURRENT - - -

COMPUTED WITH FUNDAMENTAL
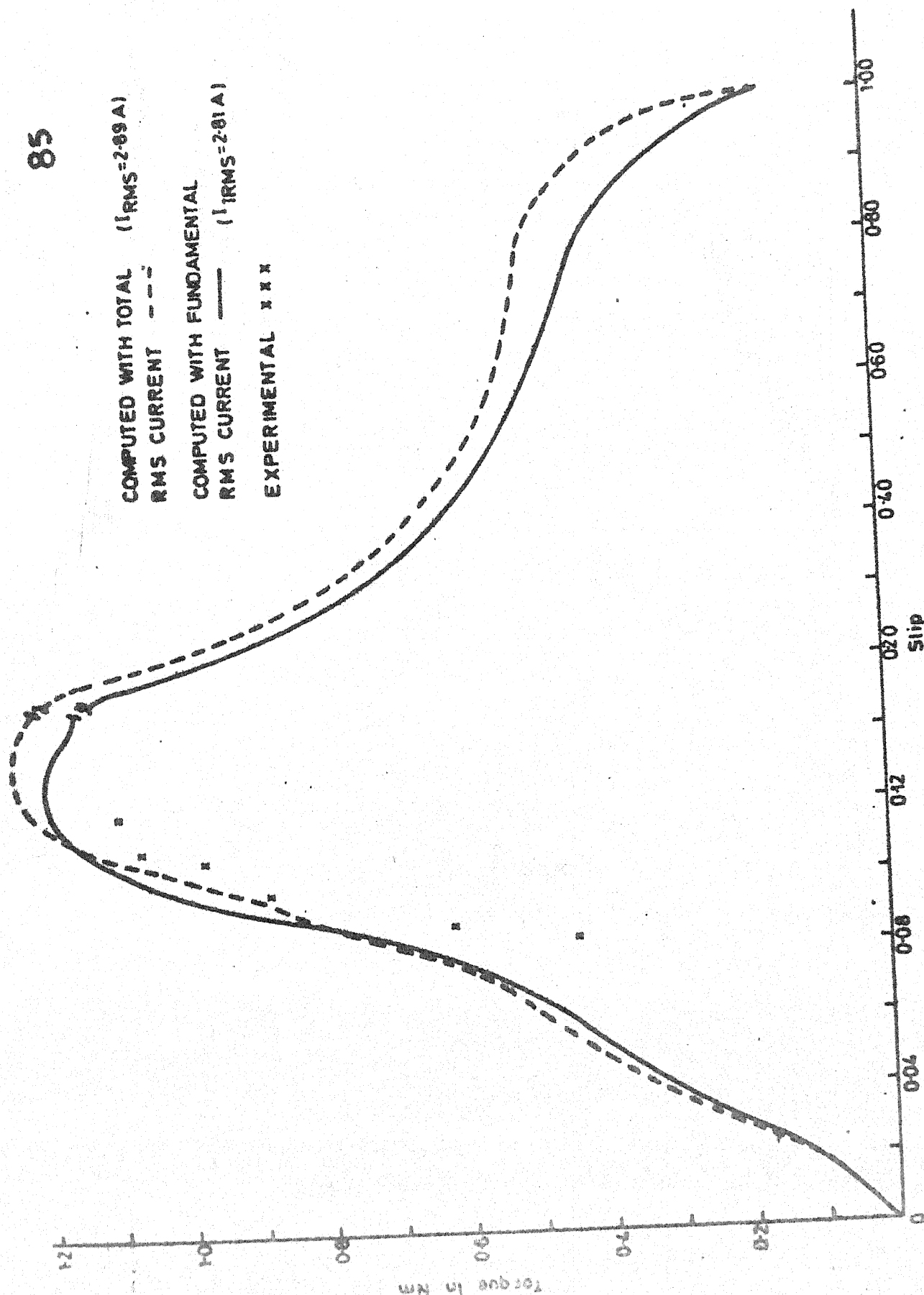RMS CURRENT ——— ($I_{1RMS} = 2.81$ A)

EXPERIMENTAL x x x

The deviation of the experimental results from the analytical values may be due to the error involved in the measuring procedures and the error in the parameters used for analysis. The other reason may be due to the assumption of the load current waveform to be a perfect square wave which is not really true in the practical circuit.

5.5 CONCLUSIONS

The analysis of the single-phase current source inverter using variable frequency is quite complex as the sequence of modes is not known before hand. But for affixed frequency, the modes remain constant with the change in direct link current. Thus the analysis for a constant frequency application becomes easier. The method of analysis suggested by W. McMurray has been used to get the various voltages and currents of the current source inverter.

The magnetizing reactance in the equivalent circuit of the induction motor which gets saturated due to current source supply.is calculated. The effect of harmonic currents on the effective torque is also discussed. The method of calculating the speed-torque characteristics is described and theoretical and experimental results are compared. It is found that the harmonics currents do not appreciably contribute to the effective torque.

CHAPTER 6

CONCLUSIONS

A set-up chopper-inverter-induction motor drive is built
for possible application to solar water pump. The function
of the step-up chopper is to deliver constant voltage/current
to the inverter even under low solar radiation levels. The
drive system operated satisfactorily in the laboratory. Due
to the non-availability of solar power source and centrifugal
pump, actual field test could not be undertaken. However, the
present study on a small model in the laboratory indicates that
it is quite suitable for water pumping applications to the
farmers.

The single-phase induction motor fed by the current source
inverter has been analysed for the torque-speed characteristics
using the equivalent circuit model. The experimental results
of the load test are compared with the theoretical values.
There appears to be close agreement between the experimental
results and analytical results obtained using only the funda-
mental component of the motor current, since harmonic currents
do not contribute much to the effective torque.

In the open loop system, the variation in source voltage
is manually corrected using the chopper duty ratio control.
Thus a closed loop study can be thought of as a future work.

With proper feedback, the link voltage or the load voltage can be kept constant. It will be interesting to perform an actual field test with the closed loop system for operational experience.

REFERENCES

(1)   Erich A. Faber, "Solar energy, its conversion and uti-
        lization", Solar Energy, Vol. 14, Feb. 1973.

(2)   E.L. Ralph, "Large scale solar electric power generation",
        Solar Energy, Vol. 14, Dec. 1972.

(3)   A.M. Zarem, Introduction to the Utilization of Solar
        Energy, McGraw-Hill, N.Y.: 1963.

(4)   V.G. Bhinde, "Conversion of solar energy into mechanical
        and/or electrical power", in UNIDO Solar Expert Group
        Meeting in Vienna, Austria. Feb. 14-18, 1977.

(5)   Karassik et al., Pump Handbook. McGraw-Hill Company,
        New York: 1976.

(6)   J. Appelbaum and J. Bany, "Performance analysis of d.c.
        motor-phovoltaic converter system-I separately excited
        motor", Solar Energy, Vol. 22, No. 1979.

(7)   J. Appelbaum and J. Bany, "Utilization of solar energy for
        electrical motor drive", in Proceedings of International
        Conference on Electrical Machines at Brussels, Belgium.
        Part II, Sept. 1978.

(8)   A. Eggers-Lura, Solar Energy in Developing Countries:
        an Overview and Buyer's Guide for Solar Scientists and
        Engineers. Pergamon, Oxford: 1979.

(9)   Arthur H. Hoffmann, "Brushless synchronous motors for
        large industrial drives", IEEE Trans. Ind. and Gen.
        Appl., Mar/Apr. 1969.

(10)   G.E. Company, SCR Manual, Syracuse, U.S.A., 1972.

(11)   M. Ramamoorthy, An Introduction to Thyristors and
        Their Applications. Affiliated East-West Press Pvt.Ltd.,
        New Delhi: 1977.

(12)   B.D. Bedford and R.G. Hoft, Principles of Inverter Cir-
        cuits. Wiley, New York : 1974.

(13)   E.E. Ward, "Inverter suitable for operation over a range
        of frequency", Proceedings IEE, Vol. 3, No.8, Aug. 1964.

(14)   W. McMurray, "The performance of a single-phase current
        fed inverter with counter emf - inductive load", IEEE
        Trans., Ind. and Gen. Appl., Vol. IA-14, pp. 319-329,
        July/Aug. 1978.

(15) S.B. Dewan and A. Straughen, Power Semiconductor Circuits.
      Wiley-InterScience Publication, John Wiley and Sons,
      New York: 1975.

(16) B. Berman, "Design considerations pertaining to a battery
      powered regenerative system", in Conf. Rec. 1970 5th
      Annu. Meet. IEEE Ind. Gen. Appl. Soc., pp. 341-346.

(17) E.A. Klingshirn and H.E. Jordan, "Polyphase induction
      motor performance and losses on non-sinusoidal voltage
      sources", IEEE Trans. Power Apparatus and Systems, Vol.
      87, pp. 624-631, Mar. 1968.

(18) J.M.D. Murphy, Thyristor Control of A.C. Motors. Pergamon
      Press, Oxford: 1973.

(19) Tung Hai Chin and Hideo Tomita, "Analysis of torque
      behaviour of squirrel cage induction motor driven by a
      controlled current inverter and evaluation method of
      torque ripple", Electrical Engg. in Japan, Vol. 97, Nov./
      Dec. 1977.

APPENDIX A

DETERMINATION OF MACHINE PARAMETERS FROM TESTS

The following tests are conducted to determine the machine parameters :

i) The d.c. resistance R_1 of the stator winding shown in Fig. 5.3 is measured by the ammeter, voltmeter method. Taking skin effect into account, R_1 is corrected by a factor of 1.6.

ii) The machine is started up and with the starting winding disconnected, the input power P_0, voltage V and current I_0 of the main winding are measured. The no-load speed of the motor is assumed to be very near synchronous speed. The test is usually conducted at rated voltage.

iii) With the machine on no-load, the applied voltage is reduced and the corresponding input power is noted. If the voltage/power curve is extrapolated to zero of the voltage, the friction and windage losses can be estimated accurately.

iv) With the starting winding disconnected and rotor locked, a reduced voltage is applied to the main winding. The input power P_1, voltage V_1 and current I_1 are noted. This is known as the short circuit or locked rotor test.

From the test results, it is now possible to calculate the approximate values of the parameters. Thus from the locked rotor test,

$$\frac{V_1}{I_1} = Z_1 = R_1' + j\ X_1' = (R_1 + 2R_2) + j\ (X_1 + 2\ X_2)$$

$$\frac{P_1}{I_1^2} = R_1' = R_1 + 2R_2$$

R_1 being known, we get R_2 from the above eqn.

$$(X_1 + 2X_2)^2 = (\frac{V_1}{I_1})^2 - (\frac{P_1}{I_1^2})^2$$

With the assumption that $X_1 = 2X_2$ i.e. stator leakage reactance is equal to the rotor leakage reactance is made, thus X_1 and X_2 are known.

Also from no-load test,

$$\frac{V}{I_0} = Z_0 = R_0 + j\ X_0 = (R_1 + \tfrac{1}{2}R_2) + j(X_1+X_2+X_n)$$

$$\frac{P_0'}{I_0^2} = R_0 = R_1 + \frac{R_2}{2}$$

and

$$X_0 = \sqrt{Z_0^2 - R_0^2}$$

$$X_m = X_0 - (X_1 + X_2)$$

Thus the complete equivalent circuit parameters are calculated.